DEVELOPMENT OF A TESTBED FOR EVALUATION OF ELECTRIC VEHICLE DRIVE PERFORMANCE

Dimosthenis C. Katsis

Thesis submitted to the faculty of the Virginia Polytechnic Institute and State University
in partial fulfillment of the requirements for the degree of

Masters of Science
in
Electrical Engineering

Dr. Fred C. Lee, Chair
Dr. Dusan Borojevic
Dr. Jason Lai

August 27, 1997
Blacksburg, Virginia

Keywords: Electric Vehicles, Inverter Fed Drives, Efficiency, Drive Cycles

DEVELOPMENT OF A TEST BED FOR EVALUATION OF ELECTRIC VEHICLE DRIVE PERFORMANCE

Dimosthenis C. Katsis

(ABSTRACT)

This thesis develops and implements a testbed for the evaluation of inverter fed motor drives used in electric vehicles. The testbed consists of a computer-controlled dynamometer connected to power analysis and data collection tools. The programming and operation and of the testbed is covered. Then it is used to evaluate three pairs of identical rating inverters. The goal is to analyze the effect of topology and software improvements on motor drive efficiency.

The first test analyzes the effect of a soft-switching circuit on inverter and motor efficiency. The second test analyzes the difference between space vector modulation (SVM) and current-band hysteresis. The final test evaluates the effect of both soft-switching and SVM on drive performance.

The tests begin with a steady state analysis of efficiency over a wide range of torque and speed. Then drive cycles tests are used to simulate both city and highway driving. Together, these dynamic and steady state test results provide a realistic assessment of electric vehicle drive performance.

TABLE OF CONTENTS

DEVELOPMENT OF A TESTBED FOR EVALUATION OF ELECTRIC VEHICLE DRIVE PERFORMANCE

LIST OF FIGURES

LIST OF TABLES

1. INTRODUCTION

Electric vehicles (EVs) have existed for over a hundred years. When they were invented, they immediately provided an economical and reliable means of transportation. However, electric vehicles were plagued by poor range and short-lived batteries. Today, a renewed interest in environment and energy independence has compelled industry and government to again pursue electric vehicle designs. These designs focus on improving the range, efficiency, and durability of EVs.

Drive system performance is an essential part of the EV. The drive system is the link between the energy stored in the batteries and the transfer of this energy to the road. A high efficiency drive system can best utilize the batteries and effectively reduce the price of owning an EV. Therefore, accurate measurement of drive system efficiency is primary concern for the EV drive system designer.

Drive system efficiency exists in two varieties for EVs. The first is steady state efficiency measured in a controlled environment over the full range of usable motor torque and speed. The second is transient efficiency or the efficiency of the drive system when the vehicle is on the road. Together, these efficiency results help to completely characterize an EV drive system.

This thesis will present a testbed for the evaluation of EV motor drive performance. This tool takes the form of a dynamometer, automated controller, and data acquisition system. The goal of the dynamometer is to provide both steady state and dynamic testing. The dynamometer begins as a simple mechanical interface between two drive systems, the source and the load. (Figure 1) The most basic test requires a steady shaft speed regulated by a load reference motor. The system under test applies the desired torque on the shaft and power is measured at all input/output points of all components of the drive system.

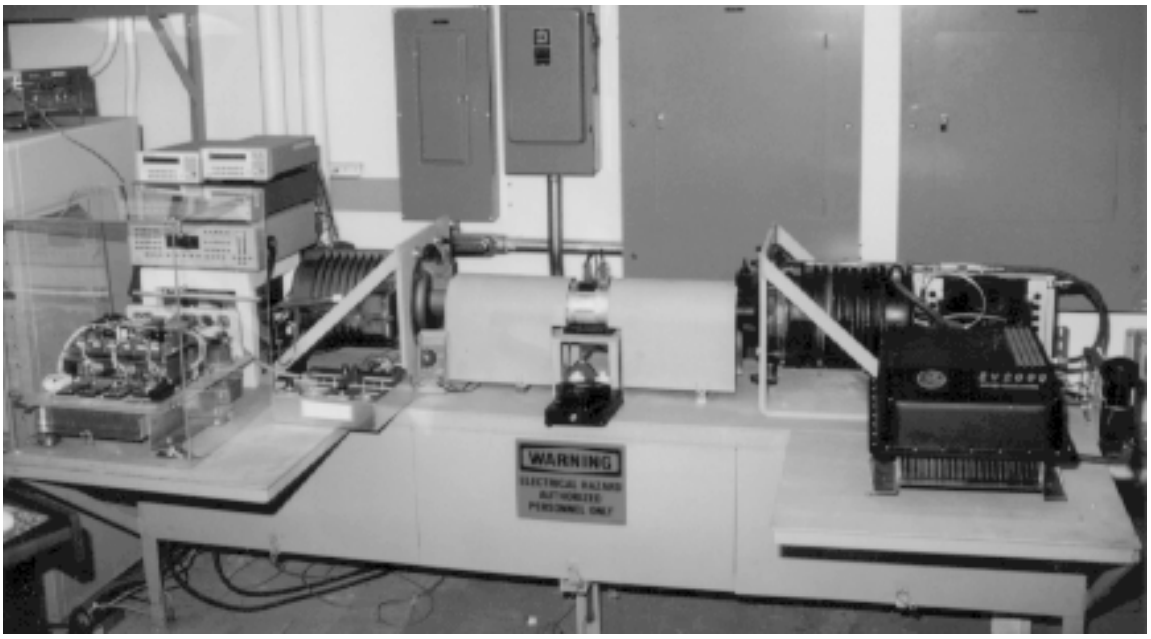

Figure 1: The Electric Vehicle Testbed

Dynamic tests use a dynamometer-computer interface to automatically control the dynamometer load reference. This automatic control changes the operating point of the dynamometer continuously. If the operating points are changed according to a drive profile, then the drive under test can experience conditions similar to on-road operation. The on-road tests use a realistic vehicle model in the form of a differential equation that includes vehicle mass, aerodynamics, tire size, and friction. Therefore, the testing done on the dynamometer table directly measures the drive system and simulates the complete vehicle using the load reference. The test results from this system should match those done if the drive system were in a real vehicle.

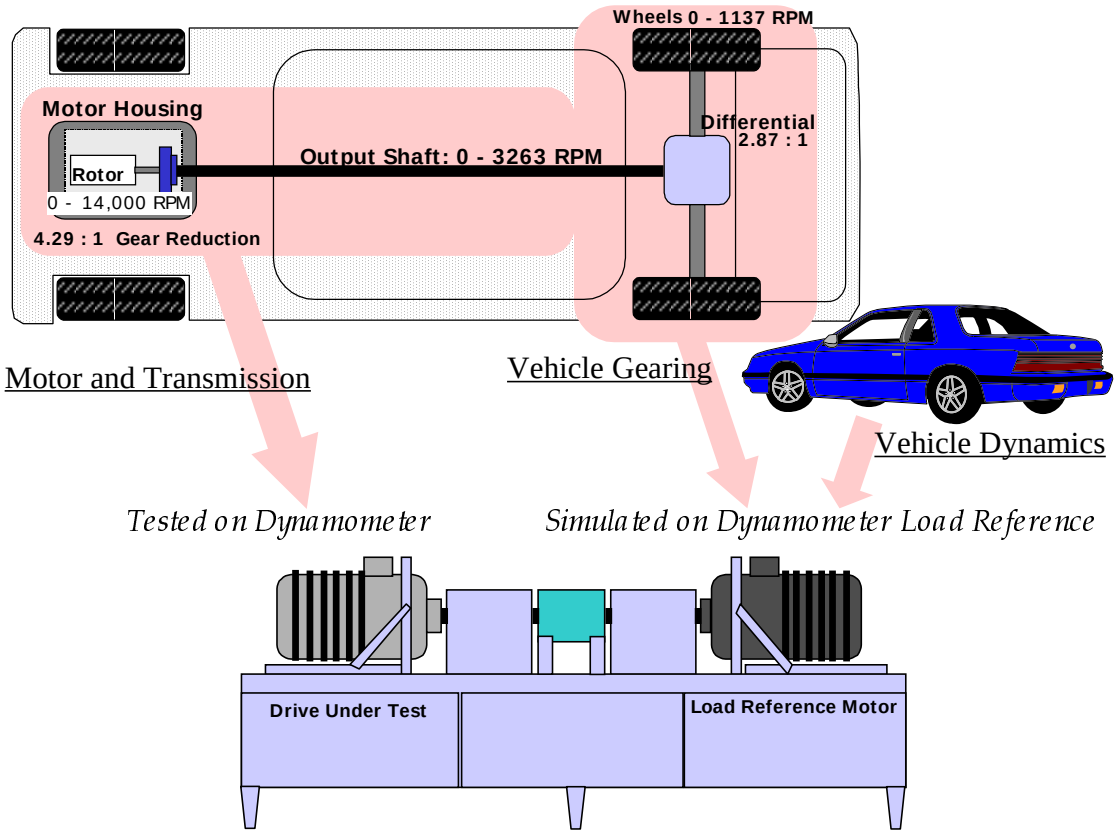

Figure 2: Drive System Test and Vehicle Simulation

Dynamometer tests must be repeatable, and accurate. To achieve this goal, a high-precision power analyzer is programmed to measure waveforms generated in a motor drive environment. Specific measurements include DC link voltage, current, and three-phase AC power to the motor. A torque computer measures mechanical torque and speed on the shaft connecting the motors. These measurements allow for a complete characterization of an inverter or motor design at 30 kilowatts continuous and up to 75 kilowatts peak.

A data acquisition program simultaneously collects, stores, and analyzes energy use over complete drive cycle programs. The program interfaces with a 16 channel, 12-bit data acquisition board. This device samples data from the torque computer, power analyzer, and inverter.

The combination of tools for steady state and drive cycle tests offers a complete platform for testing and characterizing electric vehicle drive systems. Data acquisition

brings all the data together and data analysis offers insight into the best interpretation of the data to best judge one inverter design over another.

1.1. Thesis Outline

This thesis is organized into two parts starting with **Part one**. This part covers the development of the testbed by introducing the hardware and software of the dynamometer. **Part two** presents performance evaluation data for three configurations of EV inverters. This section attempts to draw conclusions regarding the overall performance of a topology change and a modulation change.

PART ONE

Hardware use and maintenance is covered in **chapter two**. This chapter details dynamometer mechanics, control electronics, power connections, instrumentation programming, and battery management. The chapter continues with the power instrumentation of AC/DC voltage and current measurement and mechanical shaft power. The use and programming of these components is further developed.

Chapter three covers support software used in creating, executing, and data logging dynamometer tests. The first software package is a drive cycle program that uses vehicle parameters to generate automatic control files for the dynamometer interface program. The next software package is a dynamometer command-line interface created by General Electric to access the memory locations within the inverter controller and digital signal processor. This tool includes a detailed list of variables that allow the user to adjust the response of the speed reference. The third program is a dynamometer graphical user interface. This program reads the drive cycle file and sends serial commands to each inverter. Finally, data is acquired with a software and hardware package that measures analog data from the power analyzer and torque computer. The data collection software creates spreadsheet-ready text files used for motor and inverter analysis.

PART TWO

Chapter four introduces the inverters that are tested on the dynamometer. The power stage hardware, including soft-switching is introduced. Here a detailed account of soft-switch operation is offered. The next description covers the current modulation algorithms. These are current-band hysteresis control and space vector modulation (SVM).

Chapter five covers the testing and evaluation phase of the inverters. The thesis presents three tests. The first pair of inverters are based on the EV2000, A current-band-hysteresis inverter. This pair is tested with and without the soft-switching circuit enabled. The next pair uses the same hard-switched power stage, except that one inverter remains with hysteresis control and the other uses SVM. The third pair of inverters both use SVM and they are tested with and without the soft-switching circuit enabled.

Chapter six introduces the results of data collection. The steady state efficiency maps and drive cycle tests are shown. This chapter also shows the results of drive cycle energy use in tabulated form.

Chapter seven concludes the thesis with recommendations based on the results of drive cycle tests. Design strategy and driving style will impact energy use of the inverters. The conclusions will therefore discuss the most effective mode of operation for an inverter with a change in modulation or topology.

1.2. Summary

The results of the inverter testing will offer a complete picture of inverter performance for a wide range of operation. Data collected from the tests will judge efficiency improving strategies used on the test inverters. Now, more than ever, selection of topologies and modulation schemes can be optimized for each application of a new inverter. Empirical data will support the claims of efficiency improvements made to inverters whether they are topological or modulation enhancements.

PART I. TESTBED DEVELOPMENT

2. DYNAMOMETER HARDWARE

2.1. Hardware Overview and Specifications

The VPEC electric motor dynamometer accommodates the following items. (Figure 3)

1. Load and test motors
2. Dynamometer control electronics and control panel
3. Power Connection
4. Instrumentation for electrical and mechanical power
5. Dynamometer host computer
6. Electric vehicle traction battery and power supply

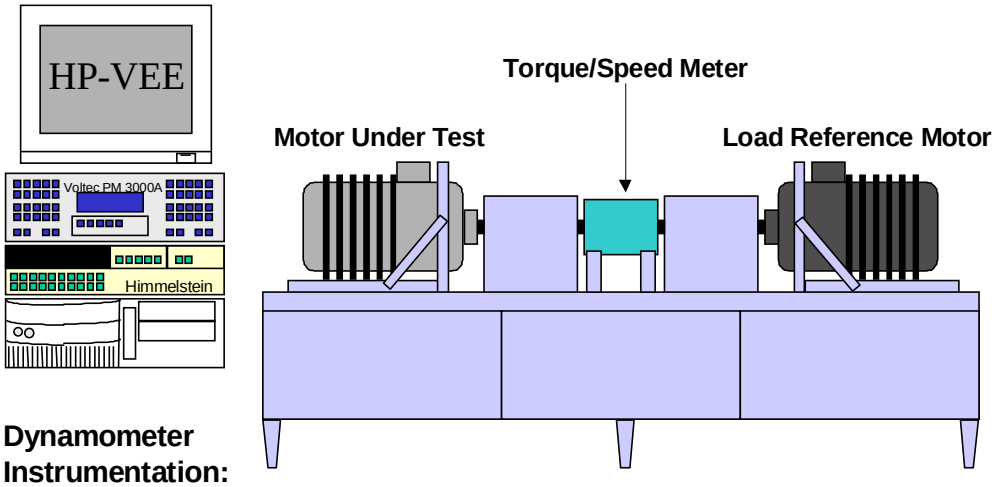

Dynamometer Instrumentation:

- Power Analyzer
- Torque Computer
- Data Acquisition Board
- Data Acquisition Computer

Figure 3: Dynamometer System Schematic

2.1.1. Load and Test Motors

The load and test motors are a high-speed AC induction squirrel cage design. The load motor is used as a shaft speed controller with the purpose of absorbing and delivering shaft power to and from the motor under test. This motor sustains continuous power levels of 35kW and temperature limited operation at 75kW. Cooling is accomplished by a closed loop circulating oil bath and a heat exchanger. The oil is sprayed upon the ends of the stator windings and into the gear-set. Then the oil circulates, cools, and filters prior to returning to the motor. The load reference motor (left), oil cooler (center, behind motor), and controller (front right) are shown below. (Figure 4, Figure 5)

Figure 4: Load Reference Motor and Inverter

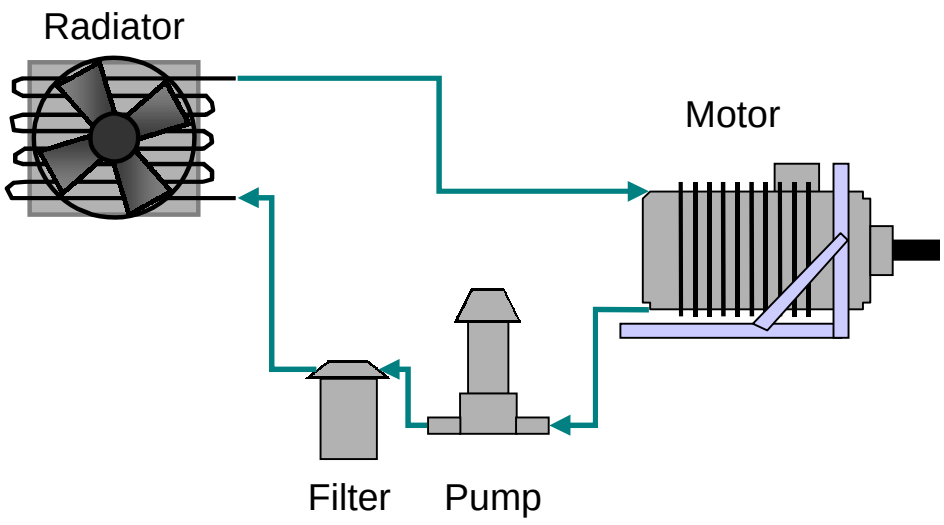

Figure 5: Load Motor, Controller, and Oil System

Rotor shaft torque can reach up to 190 NM (140 ft-lb.) at 6435rpm. Between the rotor and the output shaft, there exists a planetary gear reduction of 1:4.29. Therefore, maximum output shaft torque is approximately 813 NM (600 ft-lb.) at 1500 rpm. It is important to note that this shaft torque is twice as high as that generated by many high performance eight-cylinder automobile engines. Maximum table shaft speed is about 3260 rpm; this corresponds to about 136 kph (85 mph) in a standard automobile application. Given an average wheel diameter for a passenger car, 10,000 rotor RPM is equivalent to 96kph (60 mph). The following figure details the gearing of the drive system in a normal car and the portion of the driveline tested on the dynamometer.

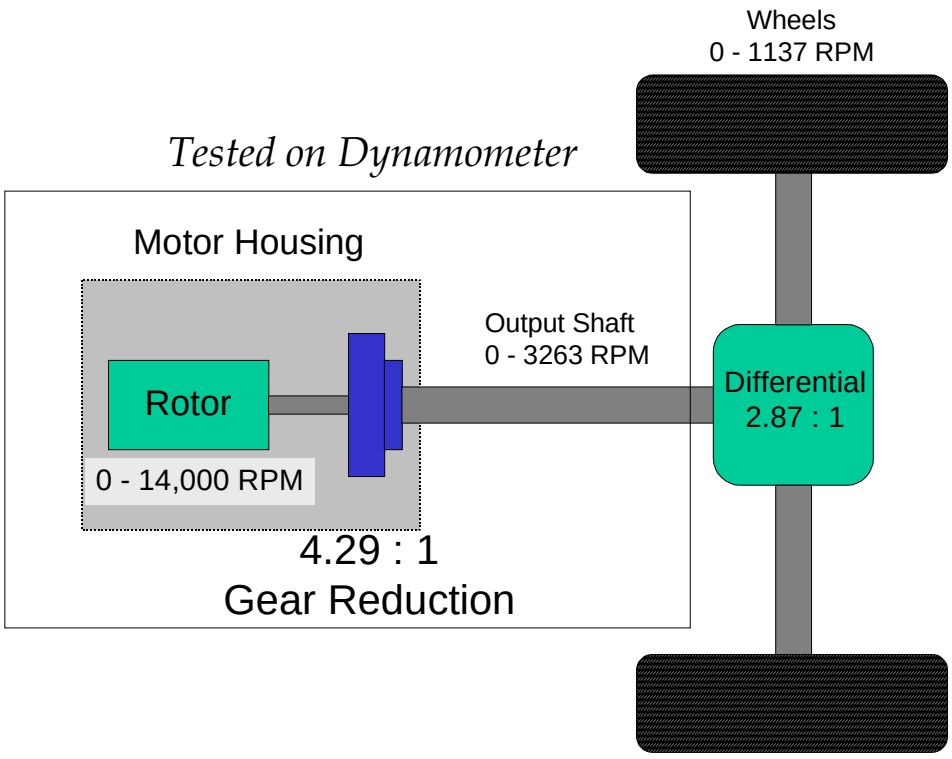

Figure 6: Electric Vehicle Powertrain Gearing

2.1.2. Dynamometer Control Panel

The dynamometer control panel provides manual control of the load and test motor. This interface gives the operator visual feedback on the state of the inverter, control over the contactors, and immediate control of torque and speed. The control panel also provides two safety shutdown options. The automatic shutdown device disconnects both the load reference and the device under test when a fault is detected in the load reference. Otherwise, only the load reference would turn-off, leaving the torque controlled inverter to accelerate without bound. Manual shutdown completely disconnects all systems from the dynamometer battery and separates the battery pack from the circuit.

The dynamometer control panel is designed to drive opto-coupler circuits located on the inverters. The necessary information exchanged between the inverters and the dynamometer control panel are:

- accelerator pedal position (transmitted as a 0-10VDC signal)

- fault status (triggered whenever a destructive fault is sensed by inverter)
- limit status (triggered whenever available power is reduced)
- ready condition (all systems and self check are functional)
- run condition (drive system enabled and/or running)

Automatic contactor control comes from the inverter asserting a “run” condition. To assert a run condition, the inverter must previously be in the “ready “ state. When ready, the operator holds a red start button and engages the main contactor switch simultaneously. This does two things, the main contactor connects the inverter directly to the DC link and a signal is sent to the inverter that the contactor is closed. If the inverter is operating correctly, it will send the run light signal acknowledging that the contactor is closed. At this time, the operator can release the start button, thus allowing the inverter to control the main contactor automatically. If a fault is measured at any time by the inverter controller, the controller will extinguish the run light. The main contactor will then open.

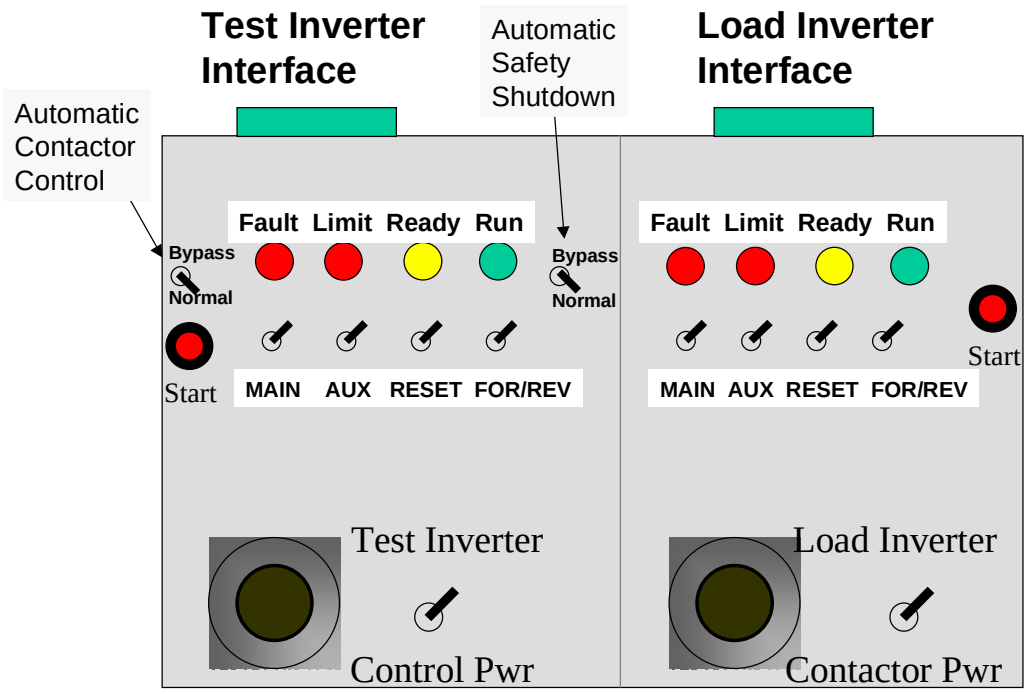

Figure 7: Dynamometer Control Panel

The most important aspect of the dynamometer control panel is that it simulates the electric vehicle interface. All the necessary controls for electric vehicle operation are covered in this interface. However, a complete inverter design used in a normal electric vehicle will also provide control signals for an external battery charger, DC-DC converter, and air-conditioning.

2.1.3. Power Connection

The electric vehicle battery-pack is used on the dynamometer to provide a high current DC link. Because a battery can absorb current as well as supply it, this dynamometer can effectively test all four quadrants of motor operation. The present dynamometer configuration connects both the load reference and drive system under test to the same battery pack. Therefore during a test, power is circulated from one inverter to

another. (Figure 8). This configuration eliminates the need for a load bank to dissipate mechanical power generated by the drive system under test.

Losses in the drive systems are made up by a parallel-connected 50-kilowatt power supply. The power supply is always connected while a dynamometer test is running, otherwise the energy stored in the batteries is slowly depleted over the course of a test. This power supply is also used for charge maintenance of the batteries

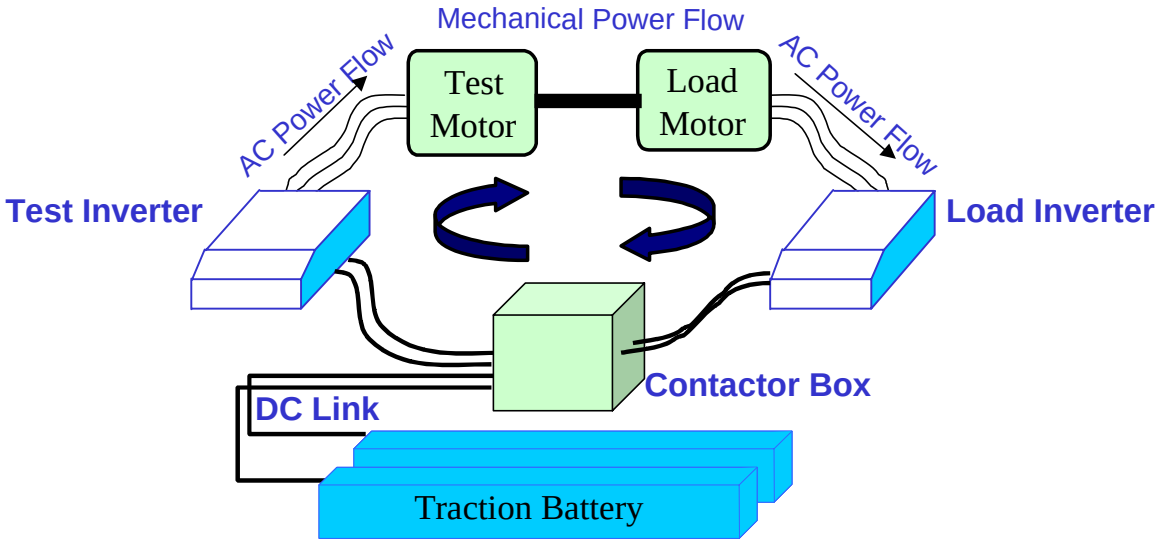

Figure 8: Power Circulation in the Dynamometer

2.1.4. Contactor Array

The contactor array used on the dynamometer connects the load and test inverters to the battery bank. This array also operates a pre-charge contactor circuit that charges the large capacitor bank in the inverters prior to direct battery connection. All the coils that control the individual contactors are connected to the dynamometer interface panel. Each contactor is designed with a magnetic blowout device to help extinguish arcing caused by a sudden shutdown under load. The specifications for the contactors are shown below. (Figure 9)

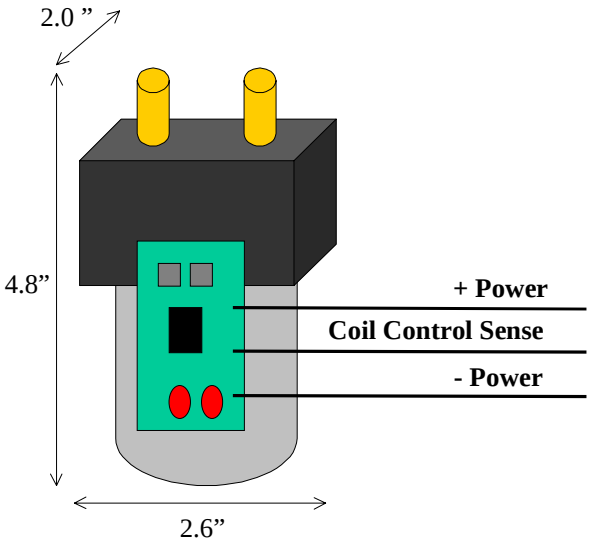

Contact Specifications:
Maximum Voltage: 335 VDC
Continuous Current: 200 A
Intermittent Current: 300 A
Rupture Current: 1500 A
Single Use Disconnect: 1000 A

Coil Specifications:
Control Voltage: 9.0 - 14.4 V
Control Current: 100 mA max
Sense Voltage: 0 = close contactor
Coil Inrush Current: 3.5 A
Coil Holding Current: 0.5 A

Figure 9: Contactor Specifications and Connections

When necessary, any device connected to the dynamometer can be disconnected through the contactor array. In the case of a severe fault, all power is removed from the contactor array. Because all the contactors operate from 12 VDC, they would all open at the command of the operator. The array then isolates each of the inverters from the battery. (Figure 10)

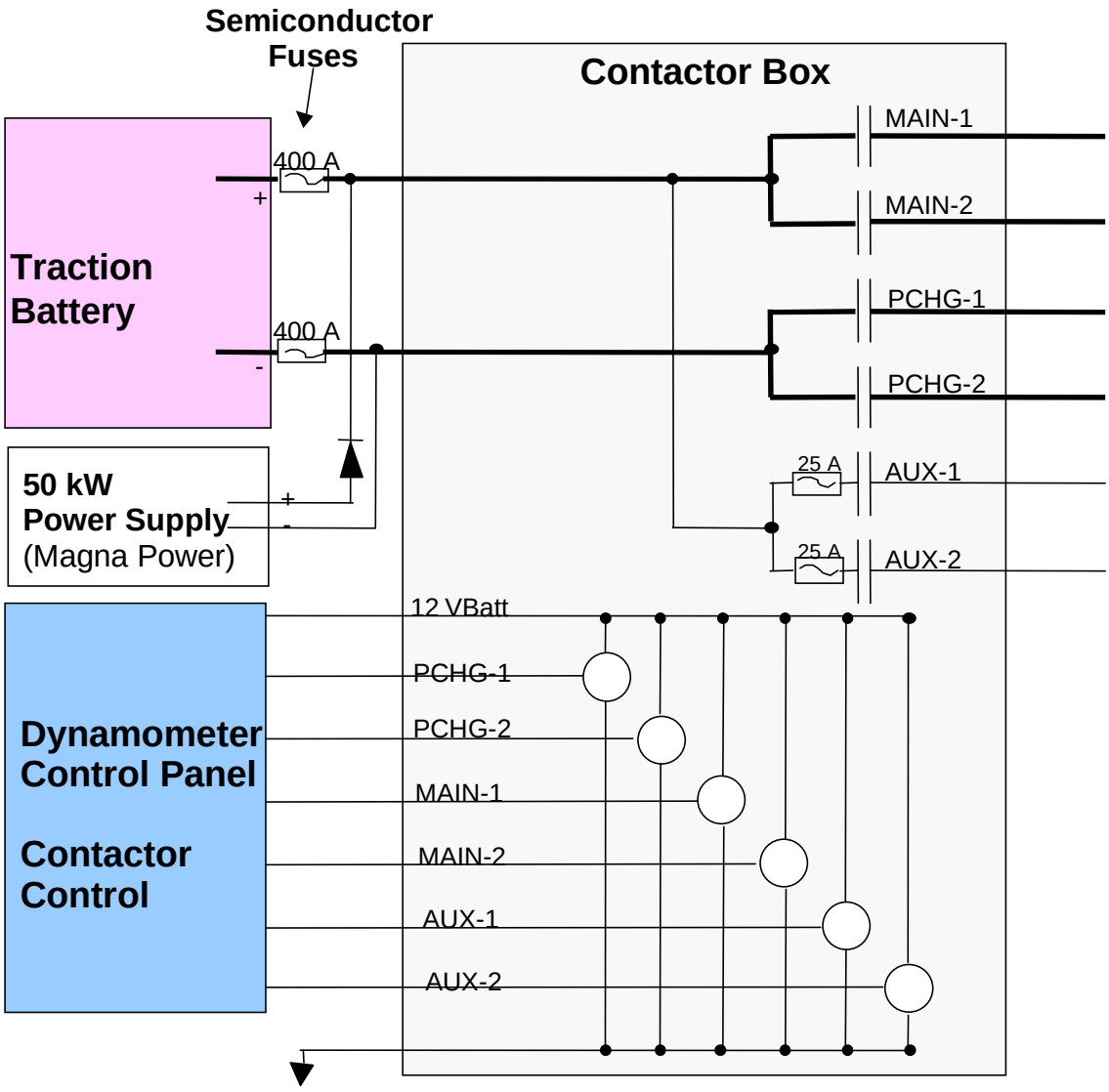

Figure 10: Contactor Array for the Dynamometer

The contactors labeled as number one are those that feed the inverter under test. The contactors labeled number two feed the speed reference inverter. The battery minus and plus contactors are connected in parallel with the 50 kW power supply. This is done to provide a common node between the two inverters, the battery and the power supply.

Because of this connection, power flows directly from one inverter to another. The battery and power supply make up only the difference due to losses. This configuration can allow testing without the need for a battery. Therefore, the operator may observe steady-state drive performance under varying conditions. This would be

done by changing the power supply voltage during a steady state test. Disadvantages of this configuration include additional voltage ripple between the two inverters and operation limited to steady state testing. However, this can be a powerful tool for analysis of the impact of DC link voltage on switching loss in an inverter.

2.1.5. Start-up Sequence

A correct start-up sequence is necessary for the inverters to charge the internal filter capacitors. Otherwise, a very high charging current would occur during battery hook-up. This pre-charge sequence is executed in the following steps.

1. Energize the 12 VDC power supplies for the dynamometer table.
2. Pull outward on the dynamometer safety-shutdown switch.
3. Turn-on the 12 VDC power switches of the test and load inverters.
4. Energize the AUX/PCHG contactor switches for each inverter and check correct operation of each inverter's controller board.
5. When both inverters are in standby (visible by moving LED light code) the main contactors can be closed.
6. Select a speed greater than zero for the speed reference of the load inverter and put the inverters in forward or reverse.

It is important to note that the motors on the dynamometer table sit facing each other. Therefore, forward motion (clockwise rotation) of one motor is opposite rotation for the other motor. To remedy this problem, a direction code can be sent to the inverters to reverse the direction of rotation. For the speed reference, this command is MICW. This command should be sent using the serial interface software discussed in section 3.2. The result of this change allows the user to run both motors in forward mode thus minimizing confusion.

2.2.Maintenance

2.2.1. Batteries

The batteries used on the dynamometer are sealed valve-regulated lead-acid (VRLA) batteries made by Hawker energy products. Each battery provides about 300 Whr. of energy storage and a low internal resistance of 6 mΩ. Short circuit current of a charged cell can reach 2000A for 10 sec. Therefore, only non-conductive tools should be dropped inside the battery box if any. The batteries are effectively no-maintenance, which only require a regular charge after use.

The low internal resistance of the batteries must be maintained to offer a stiff bus voltage under high power demand. After each dynamometer test, a recharging routine should be completed. This will help fight aging of the batteries that accelerates if the batteries are allowed to sit at a low state of charge. Figure 11 indicates individual battery voltage (shown in parenthesis) verses estimated state of charge. The complete dynamometer installation uses 26 series connected cells.

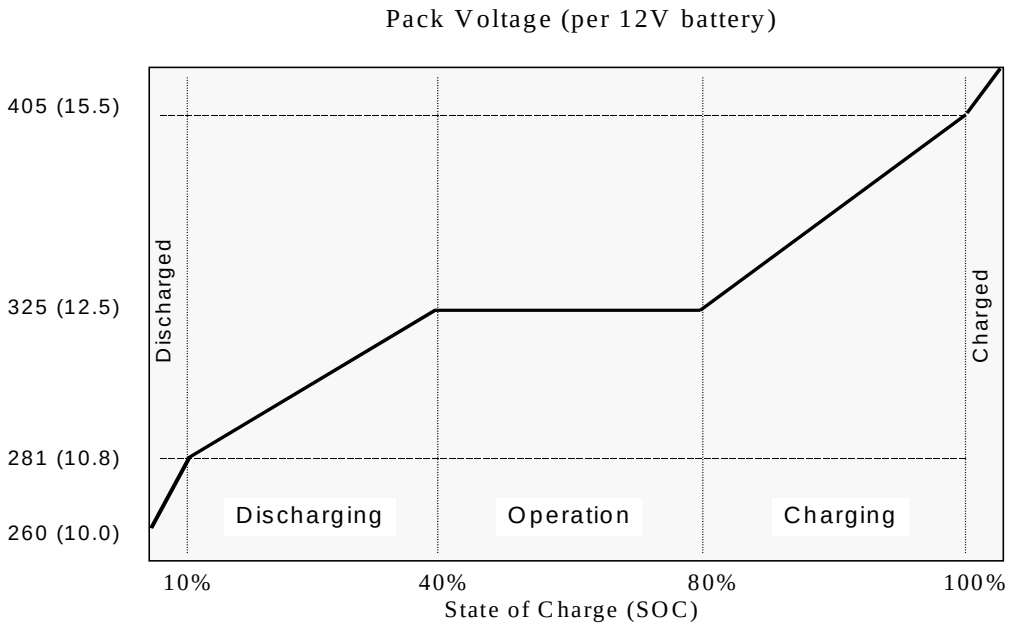

Figure 11: Battery Voltage/State of Charge Characteristic

After an extended test, the batteries should be charged after both inverters are disconnected completely from the batteries. Only the test inverter power switch should be on because it controls the battery safety disconnect contactor. With only the battery contactor enabled, battery charging can occur at a higher voltage without danger of damaging the inverters. Next, the power supply should be set to 380 volts. At this point, the battery current will read from 2 to 20 A depending on the battery's state of charge. After current has dropped below two amperes, the voltage should be increased to 405 volts. At this point it should take about an hour to drop the current to about 0.5 A. This is indicated on the power supply as the current display flashes between zero and one.

Under normal circumstances, the batteries will occasionally make a pop and subsequent whistle sound. This indicates gassing and the eventual end of the charge process. The batteries should not be allowed to gas for more than three hours as electrolyte pressure could possibly overload the gas relief valve and cause a cell rupture.

2.2.2. Mechanical Interface

The interface between the two load motors consists of a pair of double-flex Falk grid couplings connected to 1.75" diameter shafts. The grid couplings are sized to handle 6000 in-lb. continuous torque and provide three degrees of freedom to compensate for parallel, angular, and end-float misalignment along the dynamometer shaft. Each shaft terminates onto a Spicer universal joint connected to the output shaft of the motor. Between the half-shafts is connected a foot mounted torque/speed transducer. (Figure 12) This installation is the best possible because all possible misalignments are absorbed by the Falk couplings. Because the torque-meter is mounted rigidly to the table, parallel misalignment is minimized. This reduces the chance that driveline components will rotate about an eccentric axis and cause dangerous vibrations at high speed / heavy torque. Angular misalignment is handled mainly by the Spicer U-joints and end-float is absorbed within the Falk coupling.

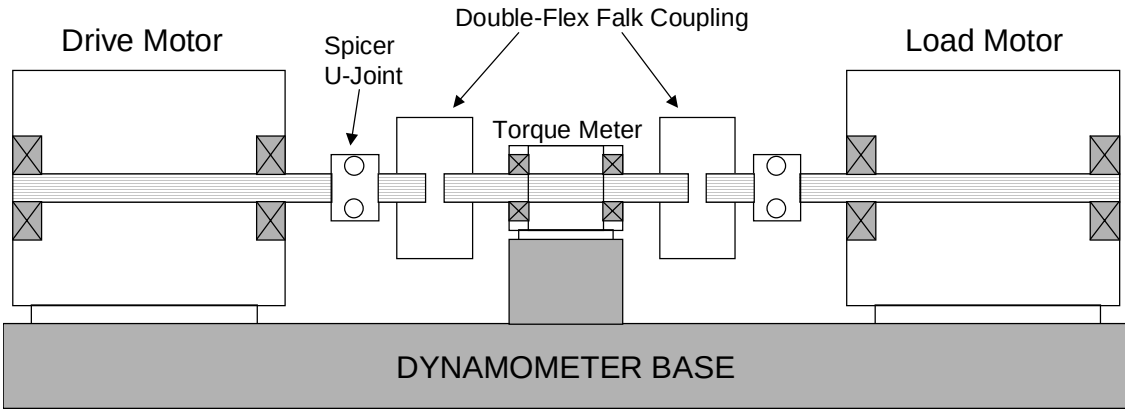

Figure 12: Mechanical Interface Components of the Dynamometer

No regular maintenance is required on the dynamometer couplings, however the Falk coupling may need to be removed when changing motors. In this case, the coupling-spring grid material should be lubricated with Falk long-term grease. The coupling set screws should mate firmly with the shaft key and Locktite brand adhesive must be used to immobilize the setscrews. This prevents the coupling from shifting along the shaft.

2.2.3. Voltage Isolation and Safety

The inverters used on the VPEC dynamometer operate electrically isolated from the steel frame of the dynamometer. Electrical isolation guarantees that both power input leads of an inverter must be exposed to a common circuit before dangerous currents can flow. An example is with stator winding faults within the motor. If the dynamometer base is isolated from the DC Link, then no current flows between the stator and batteries. This helps avoid catastrophic failures in the motor or inverter during operation.

Each inverter contains a balanced resistor capacitor network that pulls the inverter chassis to a potential of one-half bus voltage. In case of a ground-fault, this voltage balance is not maintained and operation of the dynamometer can become unsafe. A simple test for voltage balance includes measurement of the voltage of each power lead

with respect to dynamometer ground. One-half battery voltage should always be present from the chassis to either the positive or the negative side. (Figure 13)

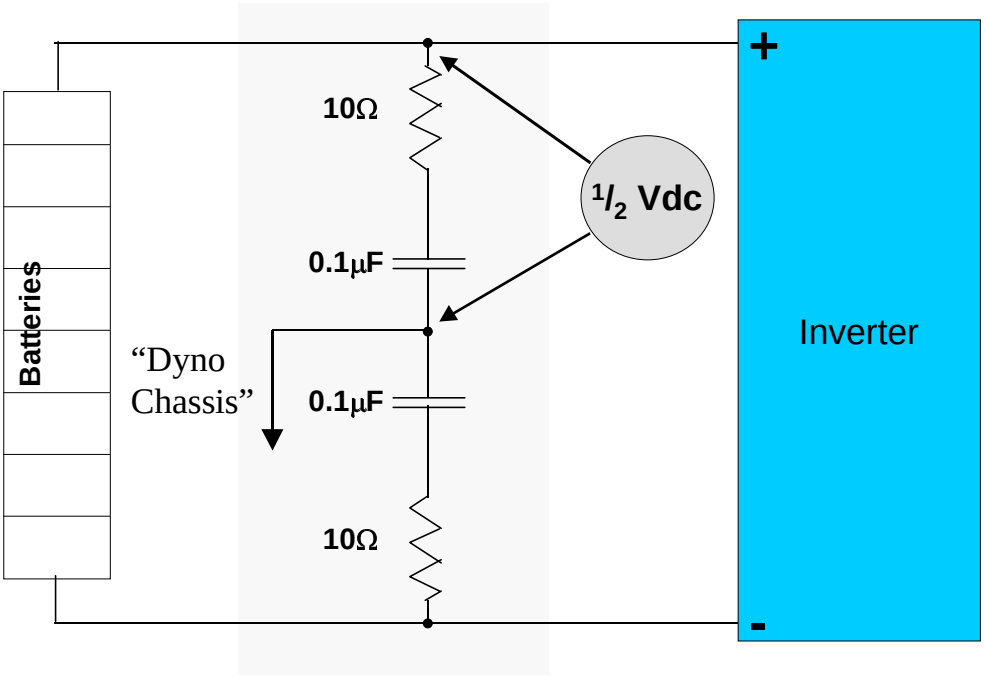

Figure 13: Measurement of Ground Balance Voltage

The power supply to the contactor array on the inverter can be manually disconnected in case of danger during operation. This is done via the dynamometer shutdown button located on the 12Vdc-power supply. When necessary, activation of this button shuts off the inverters by opening the coil power supply to all contactors. This includes a battery isolation contactor inside the battery container. If the inverters detect the fault, gating will be disabled during the opening of the contactors. This minimizes the arcing period that the contactors must sustain thus minimizing contactor damage.

2.3. Instrumentation

Instrumentation on the dynamometer is used for measuring shaft power, DC power, and AC power. All aspects of the drive under test can then be logged using a data

acquisition system connected to the torque computer and power analyzer. The collected data is logged to file on the dynamometer computer where post processing is done for efficiency analysis.

2.3.1. Torque Transducer / Computer

The torque/speed transducer is a non-contact strain gauge that measures the mechanical deformation of a solid shaft connecting the two motors. It inductively-couples to the torque computer. Maximum speed and torque ratings are 8000 rpm and 1,111 NM. The transducer hardware requires neither regular maintenance nor lubrication. A hall-effect pulse counter is also built-in to the torque meter housing for speed measurement. The pulse source is a sixty-tooth wheel mounted on the shaft. It outputs a one hertz square-wave per each revolution.

The torque computer on the dynamometer is connected to a torque/speed transducer located in the connecting shaft of the load and test motor. The torque computer is calibrated to measure shaft torque in inch-pounds from a transducer designed for a full-scale torque of 10,000 in-lb. Shaft speed is measured from a 60-tooth wheel located within the torque transducer. The display of the torque computer integrates the measured torque, displays speed, and calculates both positive and negative shaft power transfer between the motors.

Analog voltage and frequency outputs from the torque computer are connected to the power analyzer and to the data acquisition unit. The power analyzer averages and synchronizes the torque and speed signals with the motor AC power, the resulting motor power and efficiency is made immediately available for steady state analysis. The data acquisition unit provides a means for high speed sampling to a data file. Once captured, the torque and speed data is integrated over the drive cycle interval for a measurement of drive cycle efficiency.

2.3.2. Power Analyzer

The power analyzer used on the dynamometer measures AC, DC, and motor shaft power. It combines all energy measurements and interfaces to a computer for data logging. The AC and DC currents (up to 500A peak) are measured with a LEM LT-300

closed-loop hall-effect sensor. The two-wattmeter method is used to measure AC power between the motor and inverter. DC link power measurements are timed to occur simultaneously with AC power. Therefore, efficiency of the inverter is immediately calculated and more accurate than if separate instruments were used.

Finally, the motor shaft torque and speed inputs are connected to the torque computer to measure total mechanical power and motor efficiency. Because the power analyzer accepts only positive input torque, it connects to the bipolar output of the torque computer using an absolute value circuit. This circuit provides unity gain amplification and ideal rectification of the analog signal voltage that represents torque. The speed input originates from the square wave pulse generated in the shaft speed-pickup sensor.

A specific measurement mode is available on the power analyzer. It is called PWM drives mode. In this mode, the AC current waveform is filtered within the boundaries of 5 Hz to 500 Hz to isolate the fundamental frequency. This helps to synchronize the analyzer with the motor to insure correct triggering on the waveforms. An infinite-order-response filter eliminates all signals above 20 kHz. The actual RMS quantities are then captured from the unfiltered data below 20 kHz and used to calculate three-phase AC power.

The following equation shows the power measurement scheme for the two-wattmeter method.

$$Watts(channelX) = \frac{1}{n} \sum_{i=1}^{i=n} V(i) * A(i) \quad \text{where i= the ith sample.}$$

$$Three-phasewatts = Watts(Channel\ 1\ +\ Channel\ 2)$$

(1)

Output motor shaft torque is sampled and averaged in the Himmelstein torque computer. The processed torque is then sent to the power analyzer. A hall-effect speed sensor picks up a 60-tooth gear to provide a square wave of one Hertz per each shaft rpm. The speed signal pulse train is connected to the external frequency input of the power analyzer. Final shaft power is then computed using the product of the torque and speed. The power analyzer uses this data to display motor efficiency.

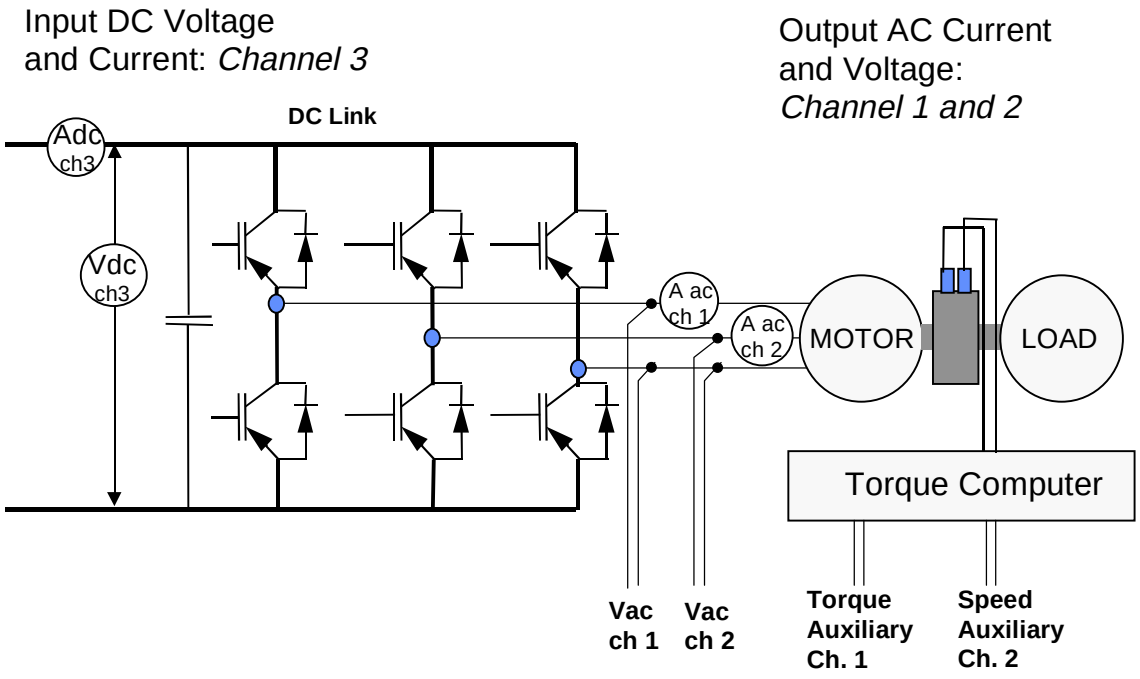

Figure 14: Power Analyzer Connection Schematic

2.3.3. Programming the Power Analyzer

The power analyzer must be set-up using the two wattmeter method this is the method used to collect the data presented in this thesis. (Figure 14) Each setting is accessible through the front panel controls. A complete system configuration is also available in printed form from the power analyzer. This outlines all the internal operating parameters that have been set to allow the power analyzer to measure PWM drive waveforms.

With a correct setup, the scaling and interface indicator should be lit, none of the wiring configuration indicators should be lit. Channel 1 and 2 should be connected to phase A and B inputs for voltage and current. Channel 3 should be connected to the DC link voltage and current.

Table 1: Power Analyzer Settings

Function	Key Programming Sequence	Result
PWM Drives Mode	F[7], mode: output, filter:5Hz – 1kHz, wiring:3 wire–3 phase	PWM drives mode with harmonic filter enabled within 5Hz to 1 kHz, Independent DC link measurement on channel 3
Scaling	Scaling Key, Voltage = 1.00, range locked, Current = 2.50, range locked, convert up	The voltage measurement remains unchanged but the current sense is scaled to reflect the use of a 10 Ohm load resistor on a 2000:1 current sensor
Integrator	Integrator Key, set time for either 25 min. or 13 min. External trigger disabled. Enable the printer, fundamentals disabled.	Used to enable integration of DC link and AC motor power. This is used to obtain transient efficiency values during drive cycle tests
Low value Blanking	F, P, [26], disable	Low value blanking displays zero Watts for the DC link during low power operation. This avoids false efficiency calculations when the chart recorder interface is used.
Chart Recorder	Interface Key, chart recorder, R1 and R2, function selection: R1: Channel 3: Watts R2: Channel Sum: Watts	This setup enables the chart recorder outputs to port power analyzer data to the data acquisition module. Used to obtain charts of inverter performance over a complete drive cycle.
Interface to Printer	Interface Key, printer, select the desired results for each channel, disable external trigger.	Used to setup the external printer for data-dump operation when the data-dump key is pressed. The power analyzer will average data on all channels and output it to the printer

3. SOFTWARE

3.1. Drive Cycle Creation Program

Drive Cycles are velocity profiles that represent a variety of different driving environments for a variety of vehicles. A common drive cycle application is the measurement of fuel economy in miles-per-gallon for new cars. Two velocity profiles are used, one imitates urban driving and the other imitates highway driving. The velocity profiles selected for this analysis are the Federal Urban Driving Schedule (FUDS) and the Federal Highway Fuel Economy Test (HWFET). (Figure 15) The FUDS cycle is a 12.0 km test that takes 1371 seconds. The HWFET is a 16.5 km test that takes 765 seconds. Average speed for the FUDS and HWFET is 31.5 km/hr and 96.4 km/hr respectively.

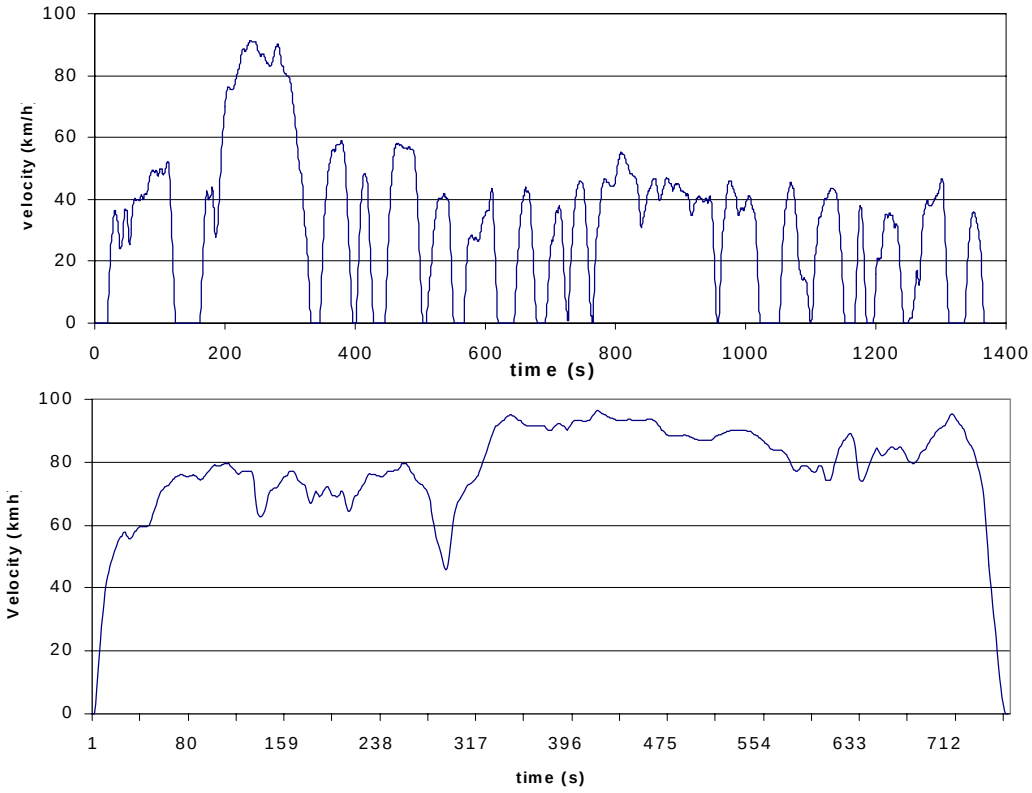

Figure 15: Federal Urban Drive Schedule (FUDS), Federal Highway Drive Cycle

When a vehicle is tested on a chassis dynamometer, it is chained down so that the tires are pressed on to drum rollers. A driver then commands torque by pressing on the accelerator pedal. The drum rollers are set to resist the rotation of the vehicle wheels based on weight and inertia. In this way, a vehicle dynamometer performs a repeatable test of the vehicle.

In the same manner, the electric motor dynamometer also simulates vehicle inertia. However, this is done without need for testing the entire vehicle. Instead, the vehicle dynamics are simulated and referred back to the drive motor in the form of additional torque. The commands for both torque and speed are then transferred via serial data communication-interface to the load reference and inverter under test. The torque command and speed command is given by the solution of the differential equation governing the dynamics of automobiles, equation (2).

$$T_{Required} = \frac{radius\left(\frac{1}{2}\cdot\rho\cdot C_{Drag}\cdot Area\cdot Velocity^{2} + Mass\cdot Gravity\cdot C_{RollResistance} + Mass\cdot \frac{DV}{Dt}\right)}{GearRatio} \tag{2}$$

This differential equation simulates the major vehicle parameters that represent the majority of frictional forces. These parameters are derived from the forces acting upon the moving vehicle and are listed below.

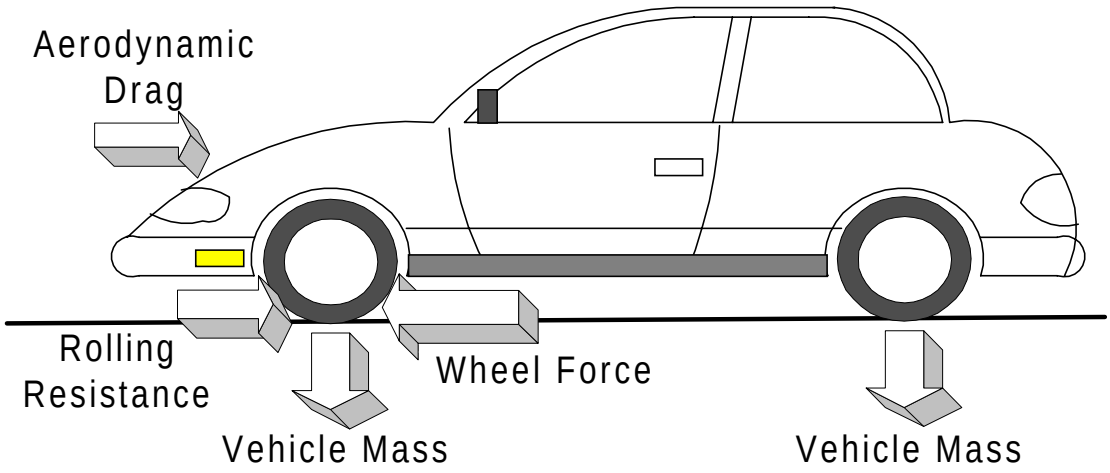

Figure 16: Vehicle Friction Force Diagram

- *radius:* radius of the wheel of the vehicle in meters
- ρ: density of air in kilograms per cubic meter
- C_{DRAG} : coefficient of drag of the vehicle body
- *Area:* frontal area of the vehicle, an aerodynamic term expressed in square meters
- *Velocity:* present vehicle speed in kilometers per hour
- *Mass:* total vehicle test mass in kilograms
- *Gravity:* acceleration of gravity in meters per second squared
- $C_{ROLLRESISTANCE}$: coefficient of rolling resistance of the tires
- *GearRatio:* constant that transposes wheel torque back to rotor shaft torque

The numerical solution of the differential equation is simple given that the vehicle speed command is given at a constant time increment. Certain speed proportional frictional constants are not present in the equation such as drive train mechanical losses. This is because they represent less than one percent of vehicle losses. In an electric vehicle, these losses are further minimized because fewer transmission components are needed compared to a conventional internal combustion engine.

The torque requirement at the wheels is divided by the gear ratio to find the torque requirement at the motor shaft. Subsequently, the given vehicle velocity data is also transposed to the motor. The result is a table of data that shows both torque and speed

referred to the electric motor shaft. The charts below show the first 150 seconds of the FUDS cycle. Motor shaft torque, speed, and power are shown below. (Figure 17)

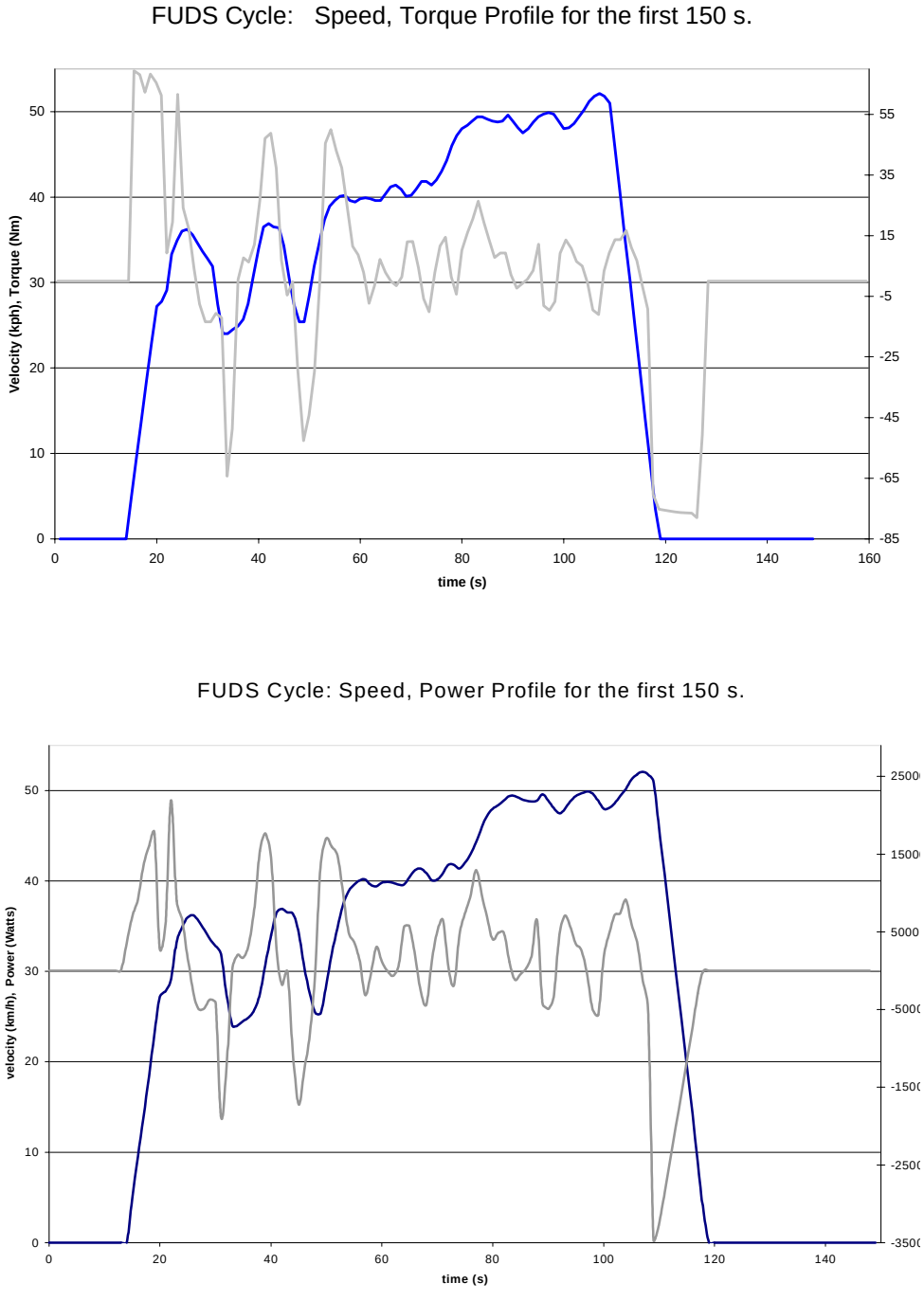

Figure 17: Speed/Torque and Speed/Power Profiles of the FUDS cycle (the first 150 seconds)

Table 2: Constants used to solve the torque equation

Air Density	1.23	kg/m^3
Accel (grav)	9.807	m/s^2
Veh. Mass	1600	kg
Frontal Area	2.2	m^2
Coef. Drag	0.42	
Tire rollres.	0.008	
Tire radius	0.32	m
Vel. m/s	0.2778	conversion from kph to m/s
gear reduct	12.3	

Torq. Equ: 0.5*CDA*rho*vel^2+mass*grav.*Crr+(mass*(delta vel / delta time)
This equation yields wheel torque, it must be divided by (gear reduction) to get the rotor torque, which is what we are interested in.

A software package was created to generate the torque and speed commands needed to create and run drive cycle tests on the VPEC dynamometer. The software allows the user to select or create an electric vehicle described by a complete parameter set. (Table 2) Then the user selects a drive cycle from a library of drive cycle files. The drive profiles and vehicle parameters are used to solve the differential equation. The solution generates a torque result that is saved with the speed data. This torque / speed table is used in the serial communication program. (Figure 18)

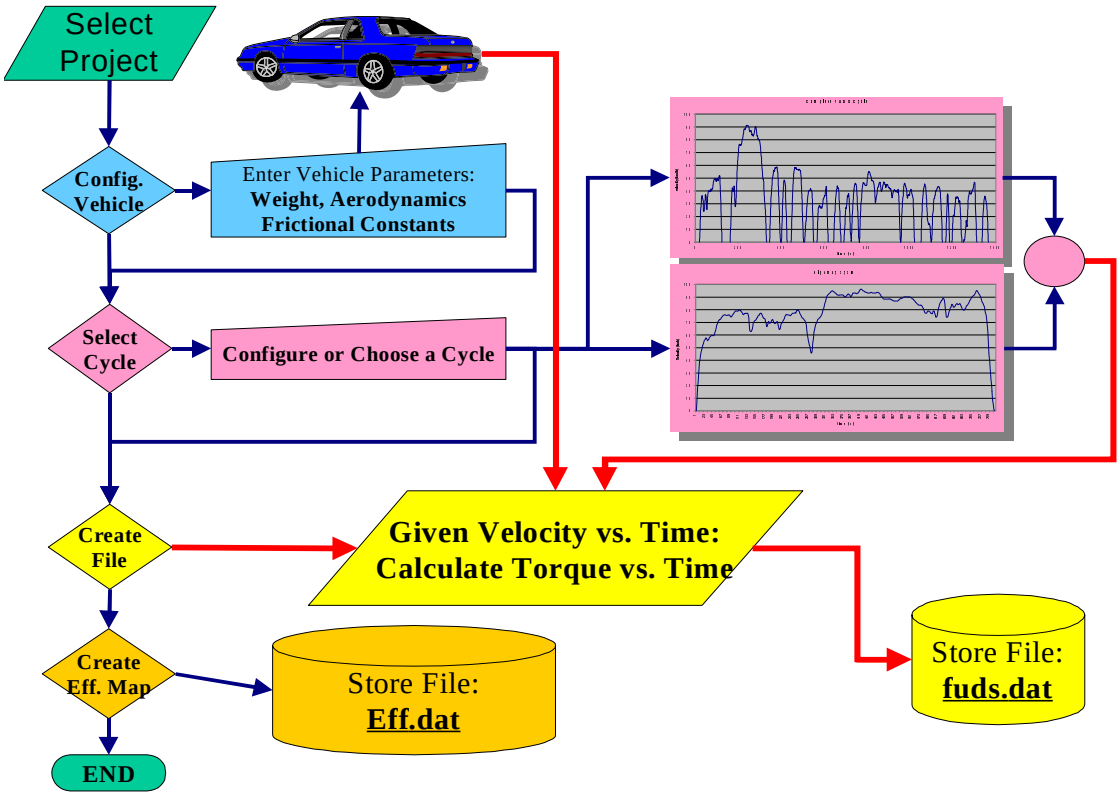

Figure 18: Flowchart of Drive Cycle Program Operation

The present vehicle parameters used in the differential equation are based on a small truck application. The primary reason for using a pickup truck is that VPEC will use one to do on-road testing a recently completed EV inverter. Additionally many electric vehicle conversions are based on small pickups since they are popular for fleet use.

The following table lists vehicle parameters for the test pick-up, a typical family sedan, and the General Motors EV1, a production electric vehicle. Note the difference in aerodynamic drag in the EV1. Aerodynamics play an important role in reducing power consumption in EVs.

Table 3: Assorted Electric Vehicle Performance Specifications

Specifications	S-10 Electric Pick-up Truck	Typical Sedan	General Motors EV-1
Mass	1600 kg	1500 kg	1364 kg
Coefficient of Drag Frontal Area (*Area*)	0.42-0.46 2.2 m^2	0.30-0.35 2.3 m^2	0.19 1.9 m^2
Wheel Radius	0.32 m	0.32 m	0.32 m
Gear Ratio	12.8	Multiple with transmission	Single, rotor to wheels: 10
Coefficient of Rolling Resistance	0.008	0.01	0.005
Peak Power	75 kW	120 kW	85 kW
Average Power	18 kW	20 kW	12 kW
Range	80 km	560 km	80 – 140 km
Seating Capacity	3 people	5 people	2 people

3.2.Dynamometer Interface

3.2.1. Speed and Torque Control Commands

The communications link to the load reference is the key to the control of the dynamometer. It is here that the commands for the desired speed are delivered. In addition, the response of the speed reference is adjustable since the operator has access to the PID controller gains located in the speed controller feedback. Specific focus is given to the command library of the speed reference. When issuing commands to the speed controller, a terminal program is used to establish communications over a 1200 baud RS232 line. The commands necessary to display or modify variables are asserted in all capital letters as “D <VARIABLE NAME>” or “M <VARIABLE NAME>”. If long term storage of the variable is desired, this is done by asserting the command “SV <VARIABLE NAME>”. This command will write the variable to the inverter’s internal EEPROM. Popular saved variables include operational defaults such as current limit settings, rotational speed limits, and tune-up variables.

The following commands cover the most popular control and tuning commands of the speed regulator [6].

- MICW: Sets the direction of rotation for the motor on the dynamometer. If it is set to zero, then clockwise rotation is the forward direction. Otherwise, forward causes the motor to rotate counterclockwise.
- MNMON: Enables the monitor mode for inverter control. When MNMON is true, the inverter will accept all subsequent commands from the RS232 interface.
- MNME: Indicates the closure of the main contactor relay to the batteries. When MNME is true, the batteries are directly connected to the inverter's DC bus. Otherwise, they are connected through a 39W power resistor.
- SMOD: Selects either speed or torque regulation as the primary operational mode, for the dynamometer load reference, this stays at "1" for speed regulation.
- MNSPD: This sets the speed reference command. Each count corresponds to 4.78 rpm or 2094 counts at 10,000 rpm rotor speed.
- ACCEL: Controls rate of acceleration to a new speed signal from the previous signal. This variable is calculated by the following equation: ACCEL = (R*10.47) / 10,000, where R is the desired rate in RPM/sec.
- DECEL: Same as ACCEL but for deceleration
- SKI: Speed regulator integral gain, reducing this value slows the response of the speed regulator. Default is 30 however, considerable vibration occurs at this setting. A value of 15 has proven well for most tests, however now the value used is 3
- SKP: Speed regulator proportional gain. This value is incremented by one half to slow the response of the speed regulator. Present setting is 200, however 400 may be better suited for drive cycle testing.
- SKLL: This is the lead/lag filter time constant used to filter the speed feedback from the tachometer. It is used to damp out oscillations in the driveline. It is presently set to 50.
- SLMF: Maximum speed limit function in forward drive mode, its sister command is SLMR, used in reverse drive mode. both are set to 2400 (i.e. 12000 rotor rpm)

3.2.2. Drive Cycle Player

The inverter serial-interface program is written in a visual programming language developed by Hewlett Packard, called HP virtual engineering environment (HP-VEE). HP-VEE is a visual programming language that allows manipulation of files, interface with laboratory equipment, and numerical analysis. The drive cycle player uses the HP-VEE serial interface structure to control the load and test inverters during a drive cycle test.

The program is designed to take a control data file created by the drive cycle program and output it to the inverters. This data file is a single column list of operating commands for both the load reference and inverter under test. The file uses the prefix S and T to identify the speed reference load and the torque reference load respectively. The drive cycle player then uses a string comparator to separate S or T prefixes and direct the subsequent torque or speed command to the appropriate inverter. A delay block is also included in the program. The delay time is read from the control data file using the D prefix and placed into a delay block. This is important because the delivery of torque and speed commands should coincide with the timing of the real drive cycle to correctly recreate the velocity profile.

The graphical user interface (GUI) of the drive cycle player contains a push button list of inverter commands that are accessed from the screen. (Figure 20) This allows one button operation for startup, initialization, shutdown, and general inverter commands. An emergency stop button on the GUI sends out a command sequence that immediately stops both the test and load inverters through software commands.

The following figure displays the flowchart of program execution. (Figure 19)

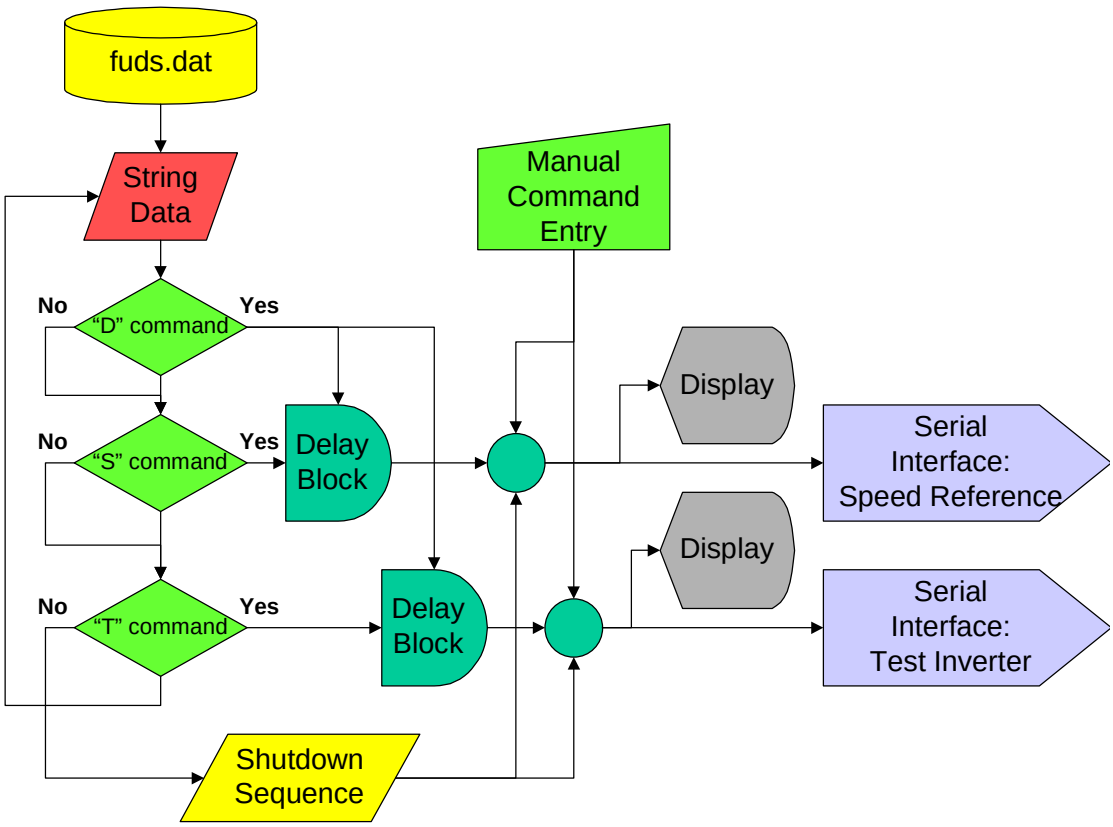

Figure 19: Drive Cycle Player Flowchart

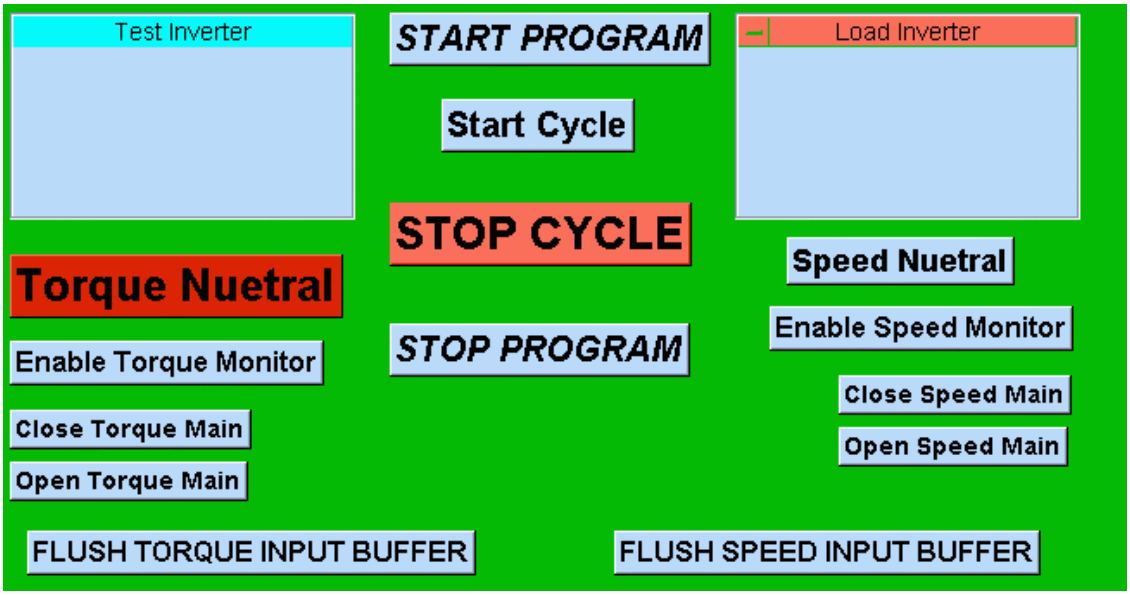

Figure 20: Drive Cycle Player User Interface

3.2.3. Data Acquisition

The data acquisition system used for drive cycle testing is based on a high-speed IO-Tech analog to digital converter hardware. This device measures data on sixteen single-ended or eight differential channels using two multiplexed twelve-bit A-D converters. Our application commands the data logger to create a four-column data list consisting of inverter DC link power, inverter AC output power, shaft torque, and shaft speed.

The interface connections to the data logger output originate at the chart recorder outputs of the power analyzer. These recorder outputs create an analog voltage that is programmed to indicate voltage, current, or power on any channel. They are scaled to take advantage of the maximum resolution of the chart recorder outputs. Our application uses 0-5 V to indicate 0 – 35 kilowatts. During a drive cycle test, these voltages are read by the data-logger's A-D inputs. The torque computer also outputs torque and speed signals to the data logger. Zero - five Volts indicates 0-10 000 in-lb. of shaft torque on channel one and 0 – 10000 RPM on channel two.

The data acquisition system is set up to acquire four hundred readings per second from each channel. Pre-triggering uses each 100 samples for averaging prior to logging one sample. Therefore, only four samples per second are logged to the data file.

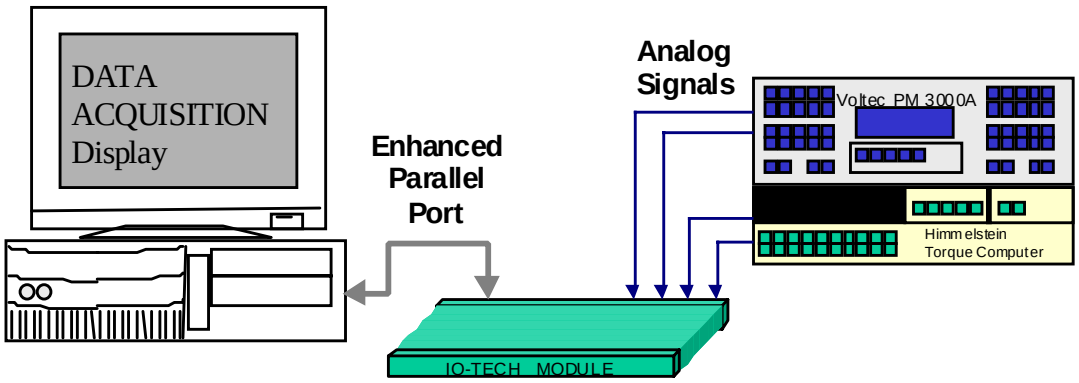

Figure 21: Data Acquisition System Schematic

PART II. PERFORMANCE EVALUATION

4. THE TEST SUBJECTS

4.1.Power Stage for the RA-94 and EV2000 Inverters

The induction motor system under test is based on the EV 2000. This is an electric-vehicle motor controller developed by General Electric. This drive was designed specifically for on-road applications ranging from light trucks to transit bus applications. Starting in February 1995, a government-funded program funded the development of an improved performance and lower cost inverter. The result of the program is called the RA-94 inverter. This inverter received two major changes over the course of the program. First, the modulation algorithm was changed from current-band hysteresis control to space vector modulation (SVM). Then a zero voltage transition (ZVT) circuit was installed to reduce IGBT switching losses. Otherwise, the new inverter uses the same vector control software and tune-up parameters as the previous inverter drive. The EV2000 inverter specifications are listed below.

- Maximum output power: 75 kW
- Maximum continuous power: 35 kW (motor thermal limit)
- Input voltage range: 220 - 380 V
- Peak current per phase: 425 A

The power stage of the test inverters use three 300A 600V half-bridge modules mounted on a forced-air-cooled heatsink. The heatsink is designed to dissipate a maximum of 1.5 kW waste-heat, while maintaining 100°C at the junction of the IGBT. A laminated bus bar structure connects the IGBT array to three 400V 5000μF capacitors. snubber capacitors are also mounted to the DC link connection directly over each IGBT half-bridge. Each capacitor is a low ESR, polypropylene type with 1 μF capacitance. They are used to eliminate voltage spikes on the DC link due to hard-switching transients and bus inductance.

The soft-switch circuit used in this inverter is based on the ZVT technique developed in [2],[3]. This ZVT technique evolved from the auxiliary resonant commutated pole (ARCP) topology [1]. The ACRP was designed to provide ZVT for a main bridge switch without increasing its current turn-off demand. However, the coupled inductor ZVT circuit is more suitable than ARCP because the coupled inductor reduces RMS current stress on the auxiliary switches. It also provides a commutation path within the auxiliary circuit to provide zero current turn-off of the auxiliary switches.

The initial application of this topology was first presented as a ZVT boost converter [4] (Figure 22). The topology was then extended to provide ZVT for three phases [4],[5] (Figure 26). The main benefits of coupled inductor ZVT in a three-phase inverter are as follows.

- Elimination of diode reverse recovery currents in main bridge prior to turn-on of the complimentary switch
- No closed loop control of the auxiliary switches required therefore the original control algorithms remain unmodified
- Zero-current turn-off (ZCT) for the auxiliary switches
- RMS current rating of auxiliary switches is one-tenth that of the main bridge switches

PRINCIPLE OF OPERATION

A single-phase inverter will be used for an explanation of the operation. (Figure 23) For the following discussion, assume that the load current, I_L, is negative (entering node A) so that the current is being switched between Dp and Sn.

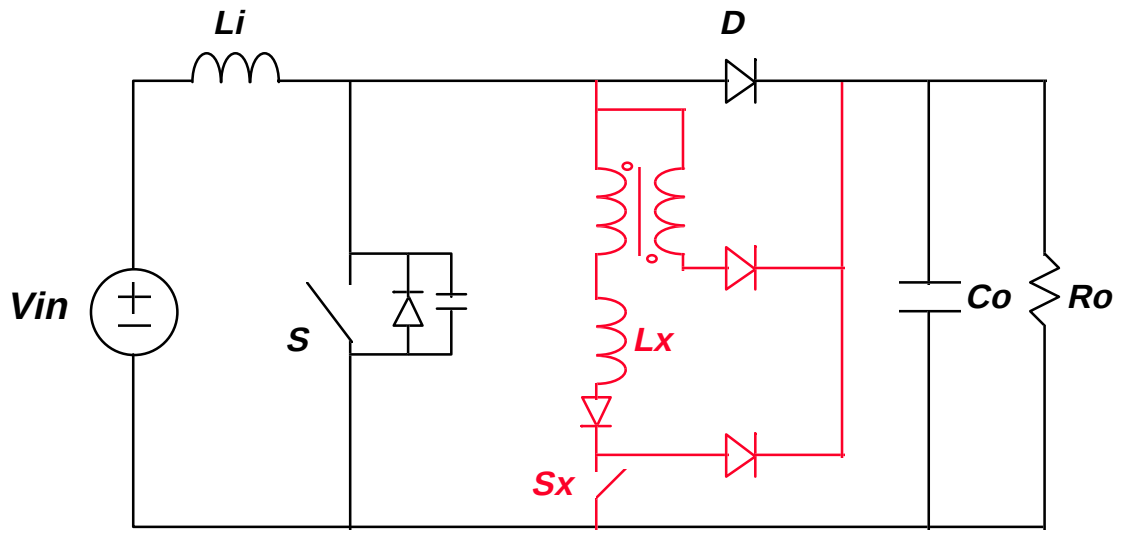

Figure 22: ZVT Boost Converter Using Inductor Feedback

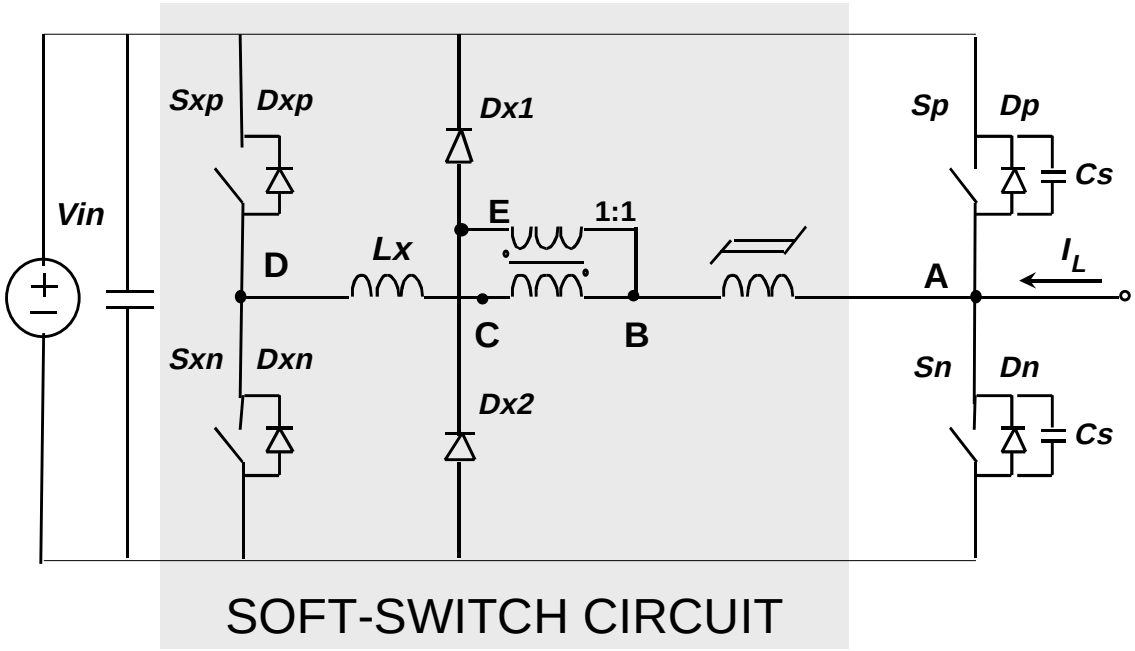

Figure 23: Single-Phase ZVT Inverter

The ZVT commutation stages (Figure 25) describe one complete switching cycle while the timing diagram (Figure 24) shows the appropriate waveforms during the turn-on process for switch Sn.

(a) **t0-t1:** Sn is conducting the load current I_L.

(b) **t1-t2:** Sn is turned off at *t1*. The load current immediately commutates to *Dp*. The voltage from node *A* to node *D* causes the saturable core to saturate. Then a small amount of current begins to flow through the auxiliary circuit. *Dxp* and *Dx1* turn on to conduct this current.

(c) **t2-t3:** Sxn is turned on at *t2* beginning the ZVT turn-on process. The DC rail voltage across *Lx* causes the auxiliary current to increase until I_{Lx} is half of I_L. The auxiliary transformer splits the auxiliary current so that I_{Dx1} is equal to I_{Sxn}.

(d) **t3-t4:** The load current has completed commutating from *Dp* to the auxiliary circuit at time, *t3*. This allows *Dp* to turn off naturally. *Lx* resonates with *Cs* until the voltage across *Sn* stabilizes at half of the DC rail voltage.

(e) **t4-t5:** *Sn* is turned on at *t4*. The voltage across the secondary side of the auxiliary transformer is reflected to the primary causing the voltage to reverse across *Lx*. *Lx* is discharged, allowing the load current to be commutated back into *Sn*. The current through *Lx* is kept from becoming negative by the magnetizing current of the auxiliary transformer.

(f) **t5-t6:** The magnetizing current of the auxiliary transformer freewheels through the auxiliary circuit.

(g) **t6-t0:** *Sxn* is turned off at *t6*. The voltage across *Sxn* rises to the DC rail voltage because *Dxp* must conduct the auxiliary transformer magnetizing current. The DC link voltage now appears at node *D*. This allows the auxiliary transformer to reset by

reversing the voltage across the windings. The saturable inductor now blocks the voltage between nodes B and A while the transformer resets.

This completes the ZVT process of the auxiliary circuit. It will remain inactive until the next switch turn-on command.

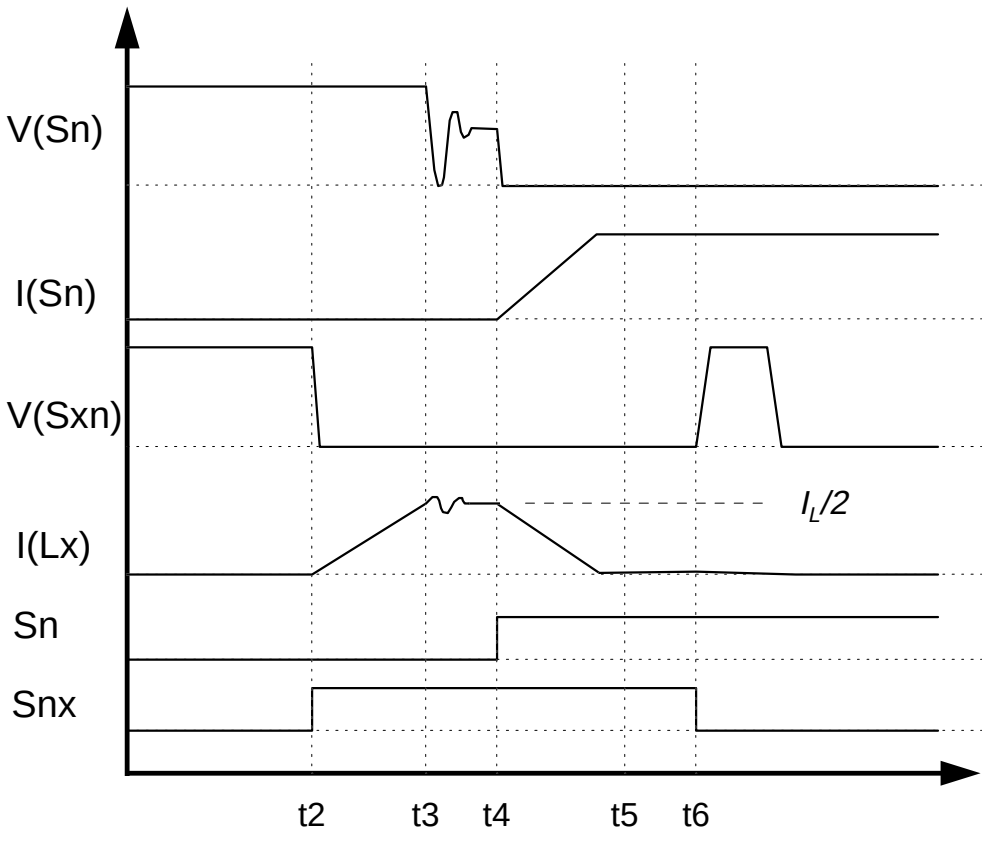

Figure 24: ZVT Turn-on Timing Diagram

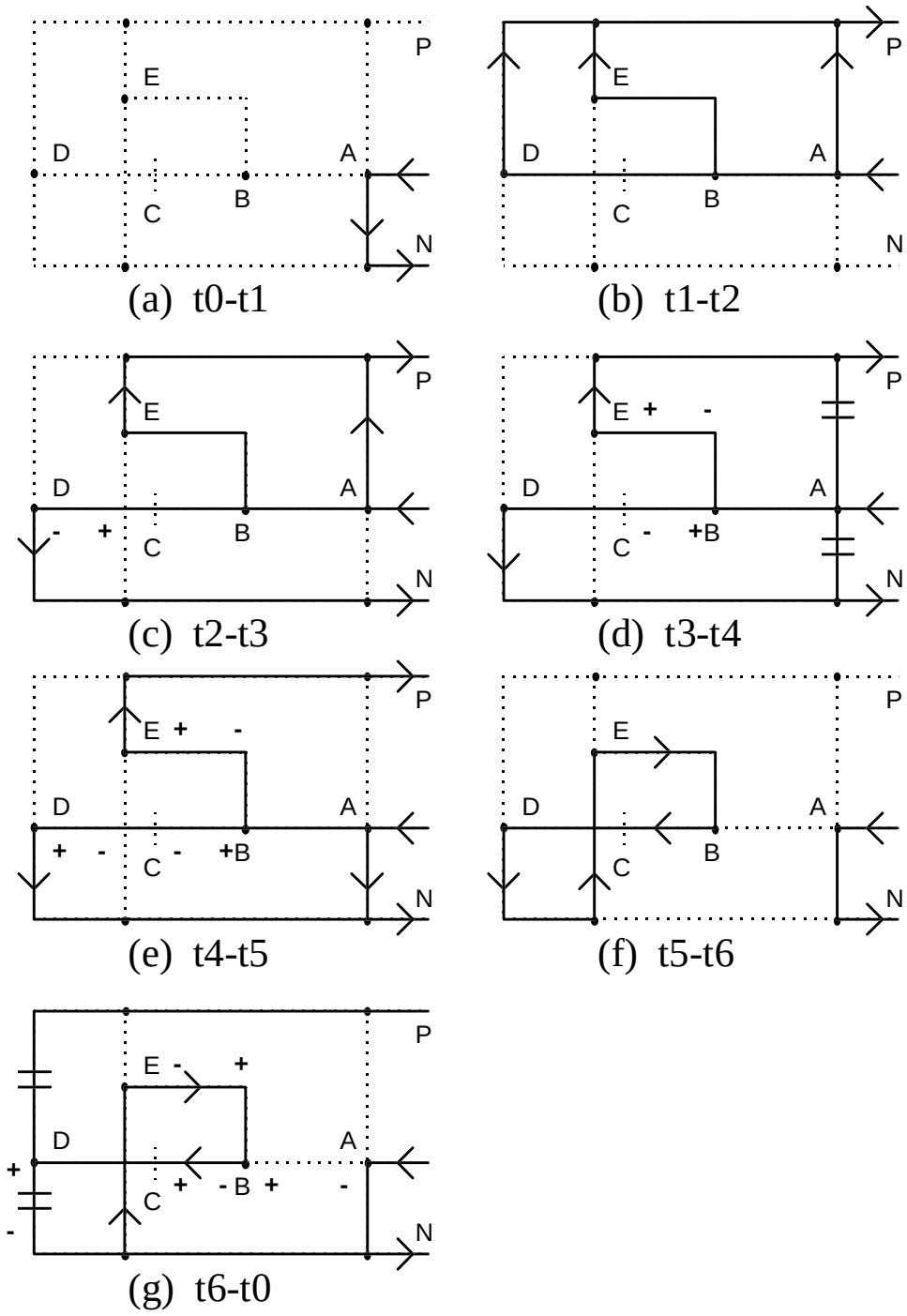

Figure 25: ZVT Commutation Stages

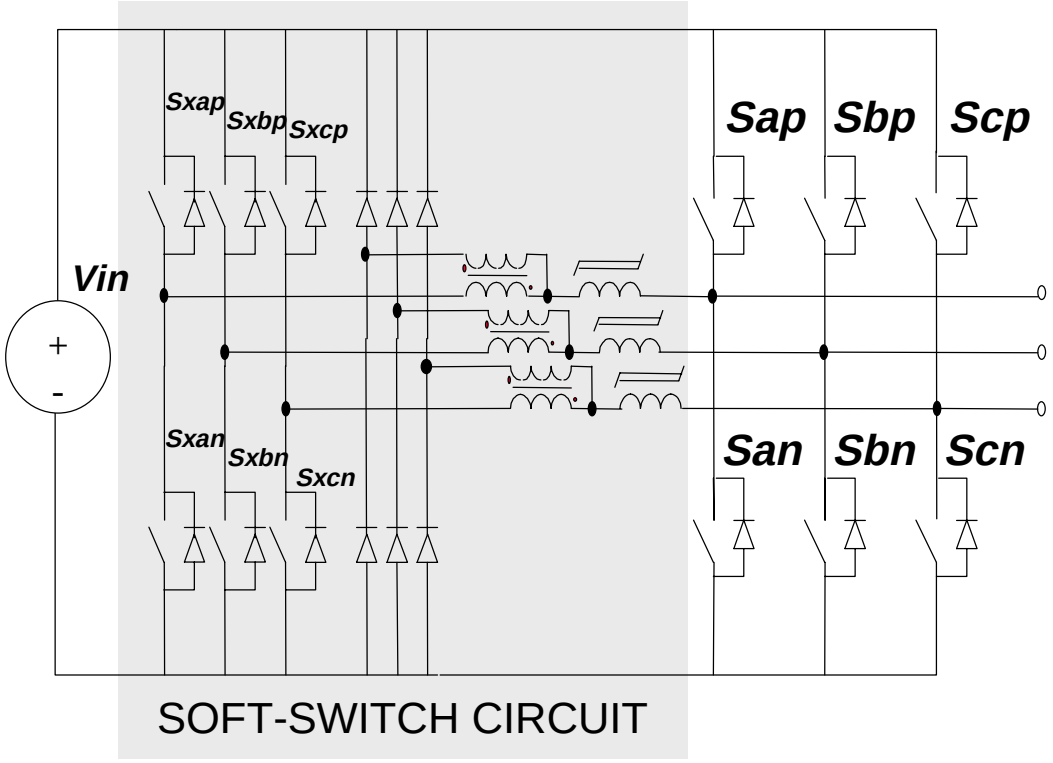

Figure 26: Three-Phase ZVT Inverter using Inductor Feedback

The following devices were used to construct the soft-switch circuit.

- Diodes: 600 V / 30 A (very fast recovery), Philips Quad-Flat Pack
- Switches: 600 V / 100 A (IGBT), Powerex six-pack IGBT
- Coupled Inductor Magnetics: 3F3 Philips Ferrite High Frequency core, ETD-49
- Saturable Core: AlliedSignal Amorphous Metal

The RMS current rating for the auxiliary circuit is less than one-tenth the main inverter bridge but the devices must sustain one-half of peak phase current at maximum power. The current waveform is essentially a narrow spike that ramps up to half main bridge current (212 Amperes) in two microseconds before the main switch transition and back to zero in two microseconds after main IGBT turn-on. The control requirement of the auxiliary bridge therefore places a fixed time pulse beginning two microseconds before the closing of the main switch and ending slightly longer than two microseconds after the closing of the main switch.

The auxiliary gate drive pulse with the timing described above is created from the original gate drive signals of the inverter using a programmable logic device. This device uses three internal counters per gate control line. When the gate command goes high, the first counter loads the initial delay time. The counter begins countdown as the auxiliary switch is commanded on. When the counter reaches zero, it loads the next delay time and commands the main switch on with the auxiliary switch still on. A new countdown from the final delay is started. Upon finishing, the auxiliary switch is commanded off, the initial delay time is reloaded, and the timer waits for the next main switch rising edge.

This gate delay technique allows the ZVT circuit to operate piggyback with almost any voltage source inverter without modifying the original control software. This is because the main switch pulse widths are not modified but only delayed by a fixed amount (2.5 μs).

4.2. Inverter Controller

The vector control software is identical for the EV2000 inverter and the RA-94 inverter. Major motor control parameters are also the same as both the new and the old inverters are optimized to drive the same induction motor. This helps guarantee that the test differences between the two inverters is based only on changes in modulation scheme and not fundamental changes in the vector control algorithm.

4.2.1. Modulation Algorithm

The EV 2000 uses a current-band hysteresis controller. This is one of the most simple and robust modulation schemes used in motor control. It requires three independent phase-current controllers that follow a sinusoidal reference voltage. If a variable hysteresis band is used, then the switching frequency can also change. This is the case with the EV 2000 inverter. It starts with a switching frequency of around 10 kHz at low speed and torque. The frequency decreases to about one kilohertz at maximum power. Eventually the inverter falls back to six-step modulation whenever the DC link voltage is too low to create the current necessary to support higher torque. (Figure 27)

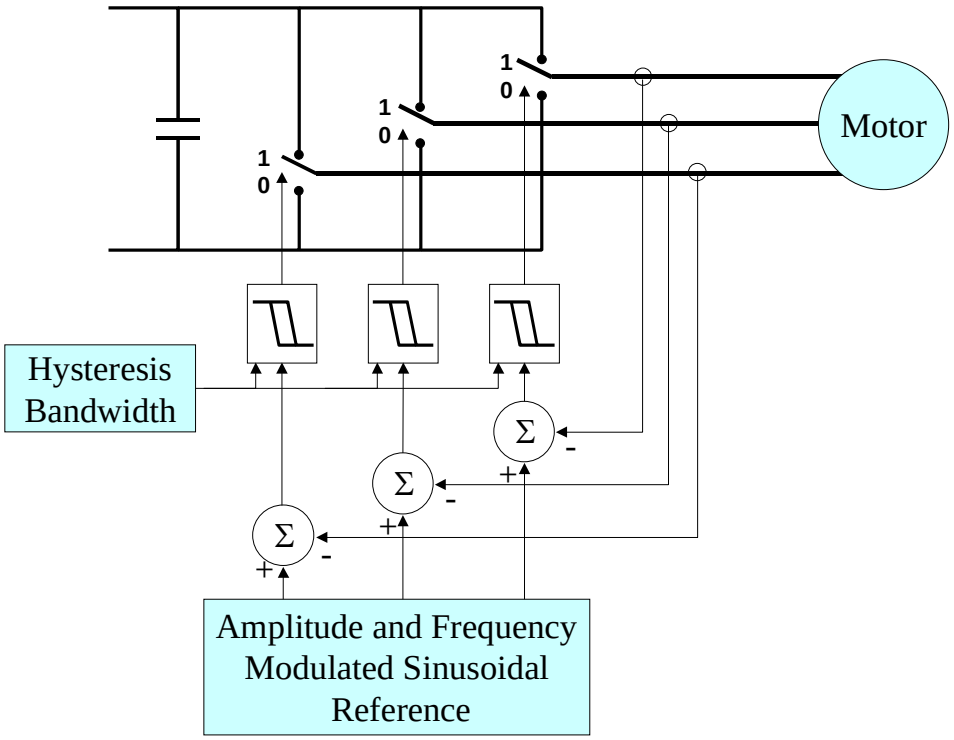

Figure 27: Current Band Hystersis Control of the EV2000

Space vector modulation (SVM) is the modulation scheme of the RA-94 inverter. SVM offers many benefits such as maximum DC link utilization for improved inverter power density, reduction in switching losses, and reduced DC link ripple.[10] SVM control requires more sophisticated control than current-band hysteresis. Vector tables containing the necessary switching sequence for each sector are a primary requirement. More logic is used to select the optimal zero vector based on the phase carrying the most current. Eventually duty cycles are calculated for each of the vectors so that the reference vector can be synthesized from the adjacent space vectors. The following figure details vector selection used in the SVM control for operation in sector I. (Figure 28)

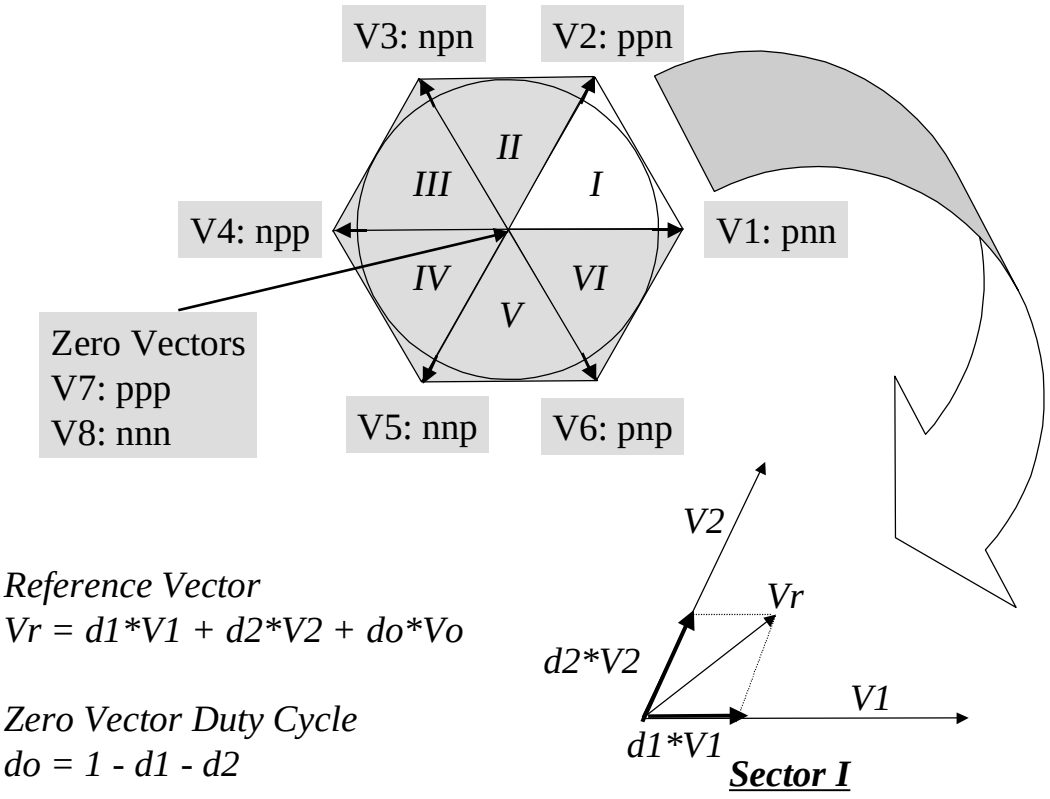

Figure 28: Vector Map for SVM (top), An Example of Vector Selection (bottom right)

The vectors in sector one are V1 and V2. A zero vector is added to make-up for the portion of the duty cycle not used by V1 and V2. This zero vector alternates between V7 and V8. Therefore, the switching sequence over two switching periods in sector one is V1-V2-V7-V2-V1-V8 for symmetrical SVM. The resulting reference vector is faithfully synthesized using this technique. However, the number of switch transitions are still high. Therefore this SVM technique offers low harmonics in exchange for increased switching losses compared to current-band hysteresis.

Optimal SVM may be used because the soft-switching topology used in the RA-94 inverter does not interfere with main switch control, (Figure 29). In optimal SVM, the number of switch transitions is limited to four within a fundamental current cycle. The combination of minimized switching with intelligent zero vector selection can reduce switching losses by as much as 50%, if load power factor is high.

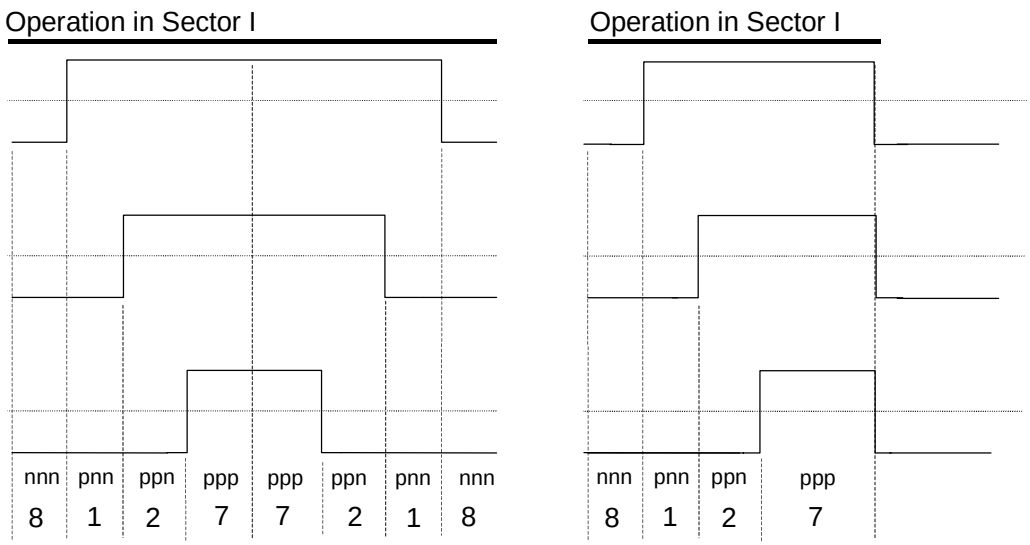

Standard SVM
•minimum harmonics
•switching transistions: 6
•symmetrical switching sequence

Optimal SVM (DD Sequence)
•moderate harmonics
•switching transistions: 4
•asymmetric switching
•extra logic used to select the optimal zero vector

Figure 29: Space Vector Modulation Methods

Even with higher harmonics than standard SVM, there is still a measured improvement in motor and inverter efficiency. This can be attributed to the reduced conduction losses in the inverter bridge. The current waveforms with SVM are close to ideal sinusoids, much unlike the current waveforms of the hysteresis controller. The absence of peaks in the phase current waveform therefore reduce current stress on the main bridge switches. This allows the main bridge losses to be much lower than hysteresis control although the average power of both SVM and hysteresis is equal.

5. DATA COLLECTION

5.1. Test Procedure

Two pairs of inverter configurations are tested on the dynamometer. The first pair of inverters use current-band-hysteresis modulation. However, the two inverters are different because one is hard-switched and the other is soft-switched. The second pair of inverters use the same power conversion topology but are different because one uses current-band-hysteresis control while the other uses space vector modulation (SVM). A third pair is introduced later to examine the effects of soft-switching on a SVM inverter. (Figure 30)

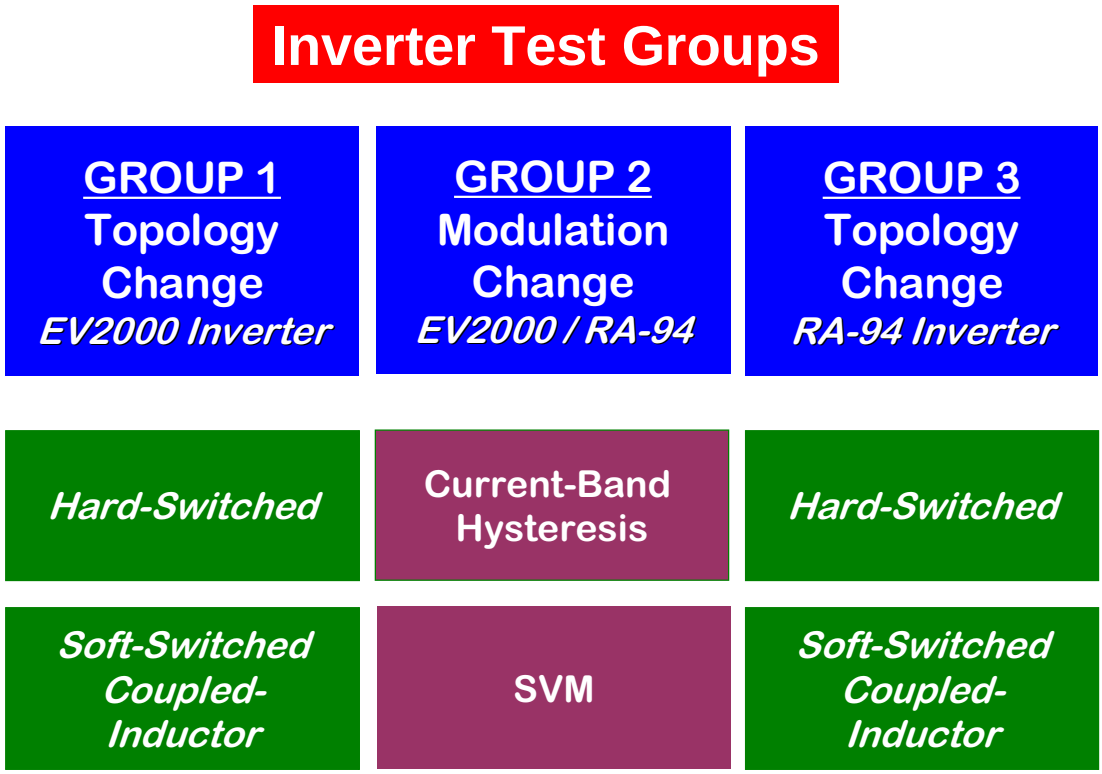

Figure 30: Inverter Test Groups

Evaluation of the inverter performance requires two steps. The first procedure is to map the efficiency of each different inverter over a complete range of torque and speeds. This work requires data on DC input power, AC output power, and motor shaft power. To collect the data, the speed inverter is set to a desired speed, and the load inverter is set to a desired torque. The power analyzer then averages 32 consecutive steady state AC, DC, and shaft power readings. This averaging process requires about 30 seconds. The resulting averages for the particular steady state operating range are then output to the printer. Subsequent data collection at the same speed proceeds quickly as only the torque reference needs to be changed.

The selection of test points is designed to maximize the number of measurements taken in places where motor and inverter efficiency changes are greater. At high power levels, efficiency results change slightly from one operating point to another. Therefore, data is collected in intervals of 13.5 NM (10 ft-lb.). At light torque, measurements occur at intervals of 1.35 NM (1 ft-lb.). In this way, a steady state efficiency characterization occurs with the need to collect only about 100-130 data points. The typical concentration of collected data points is shown. (Figure 31) The collected data provides insight into inverter efficiency over a wide range of torque and speeds within the inverter's rating. In addition, the collected data points are within the range of operation required by both the FUDS and Highway drive cycles.

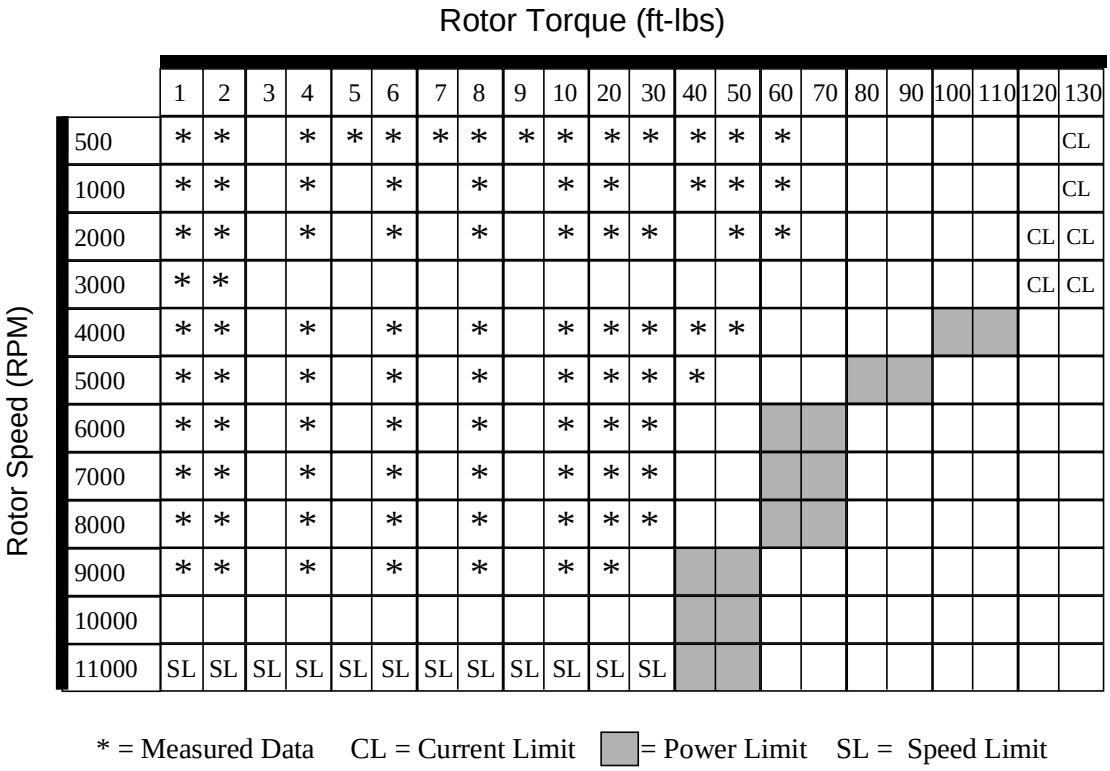

Figure 31: Torque-Speed Data Collection Map

Two arrays are prepared from the data points shown in the figure. First the inverter and motor efficiency points are calculated and inserted into the appropriate rotor speed and torque positions. Vacant positions between the collected data points are then linearly interpolated. These interpolations fill the spaces between in the efficiency points in each row. The next interpolations span between rows to fill in the empty column entries.

After the interpolation, an array of measured efficiencies is now available for plotting in a spreadsheet or in MATLAB. Actual measured and interpolated efficiency is illustrated in the form of a three-dimensional plot of torque, rpm, and efficiency.

The next step is to measure inverter performance in real driving. The FUDS and Highway driving cycles are used to subject the inverter to a driving environment on the dynamometer table. Data collection from the dynamometer is automatic during a drive cycle test. The data acquisition unit logs power continuously to a file over the course of the test. The file's data points are then averaged in a spreadsheet to obtain an overall

average power during the cycle for each component. From this data, the efficiency for each component is available. A data collection example for the FUDS and Highway cycles is shown. (Figure 32) These plots show all the torque and speed operating points encountered in each case. The important observation to make from these plots is the location of the highest concentration density. It would seem that a drive system could be optimized to operate within the most used regions, thus maximizing efficiency.

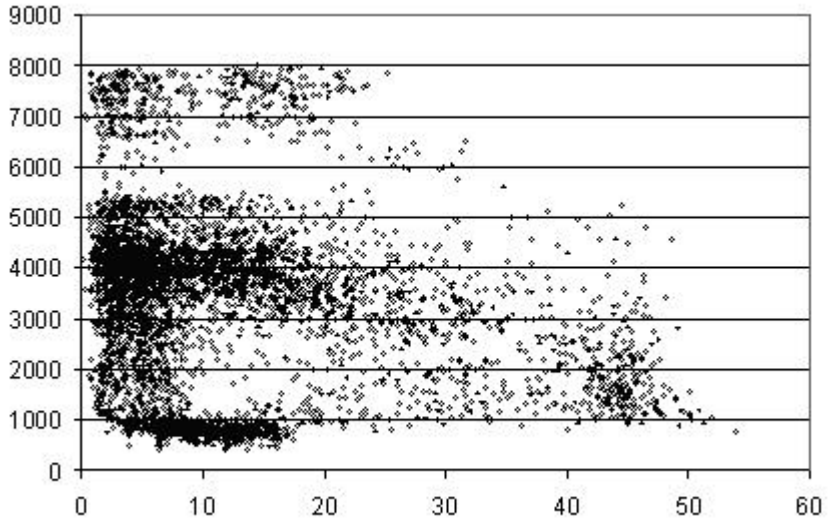

FUDS Drive Cycle Operating Points

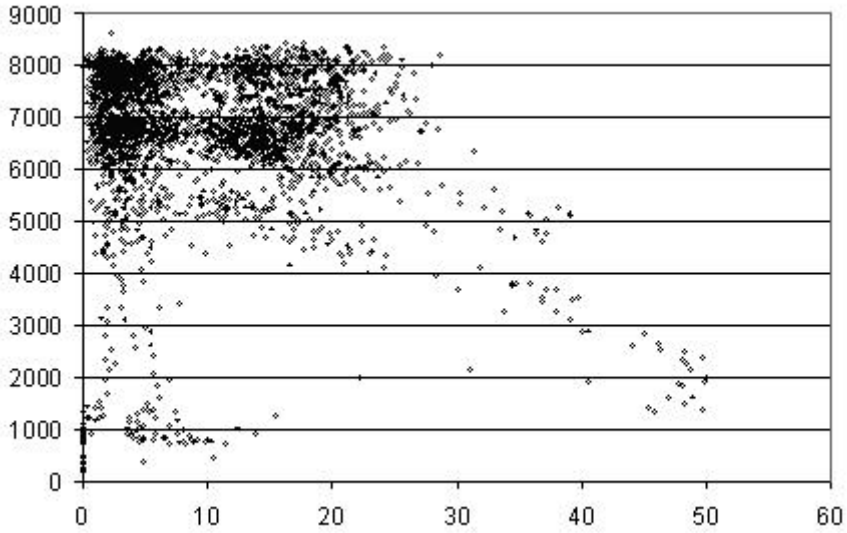

HWFET Drive Cycle Operating Points

Figure 32: Drive Cycle Operating Point Distribution

Transient inverter efficiency is a result of the drive-cycle output energy divided by the input energy. The efficiency result gives a more realistic performance measure of the inverter within its intended application. This is because the inverter input/ouput energy is integrated over the entire length of the drive test.

The drive cycle and vehicle parameters can be changed to find an optimal operating point for the inverter and motor. This analysis therefore offers the drive designer the ability create an inverter that is optimized for a specific vehicle type or road application.

6. ELECTRIC VEHICLE DRIVE PERFORMANCE

This section presents the steady state efficiency maps of the inverters and motors for each of the configurations. In each case, the inverter and motor efficiency is mapped over torque and speed. Then the inverter is changed and the identical tests are run again. Next, the inverters are compared based on drive-cycle energy use. Each inverter executes the federal urban driving cycle and the highway driving cycle. These results are then tabulated and the results are shown in terms of efficiency improvement. The following test groups are used to make the two fundamental comparisons.

- Topology modification of a current hysteresis inverter to operate with either hard or soft switching
- Modification of an inverter to control motor current using either current-band hysteresis control or space vector modulation
- Topology modification of a SVM inverter to operate with either hard or soft switching

6.1. Topology: Soft-Switching vs. Hard Switching in a Current-Band Hysteresis Inverter

6. 1. 1. STEADY STATE TEST RESULTS

This section begins with steady state efficiency measurements of the inverter and motor. Steady state efficiency data for both the inverter and motor is shown using contour plots. The first plot shows the base-line hard-switched EV2000 inverter. (Figure 33) This is followed by soft-switched inverter efficiency. (Figure 34) A difference is taken between inverter efficiency using soft switching and hard switching. (Figure 35)

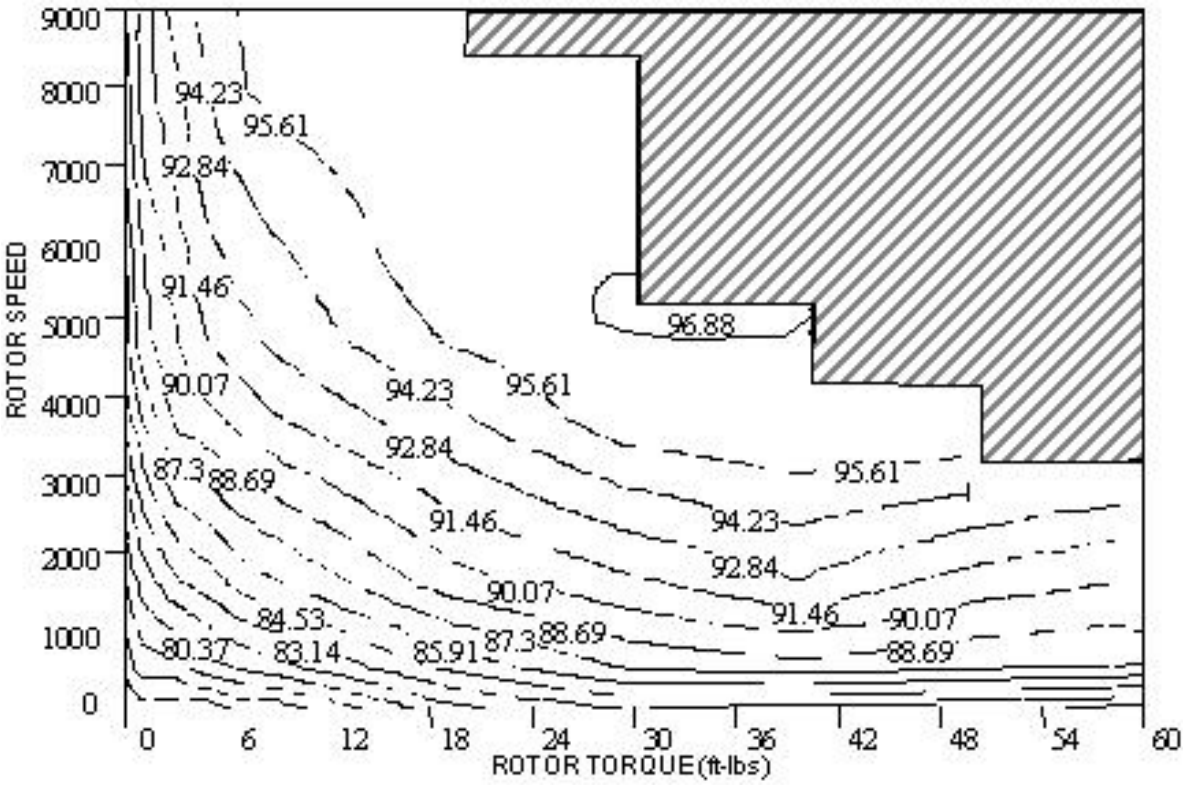

Figure 33: EV 2000, Hard-Switched Inverter Efficiency

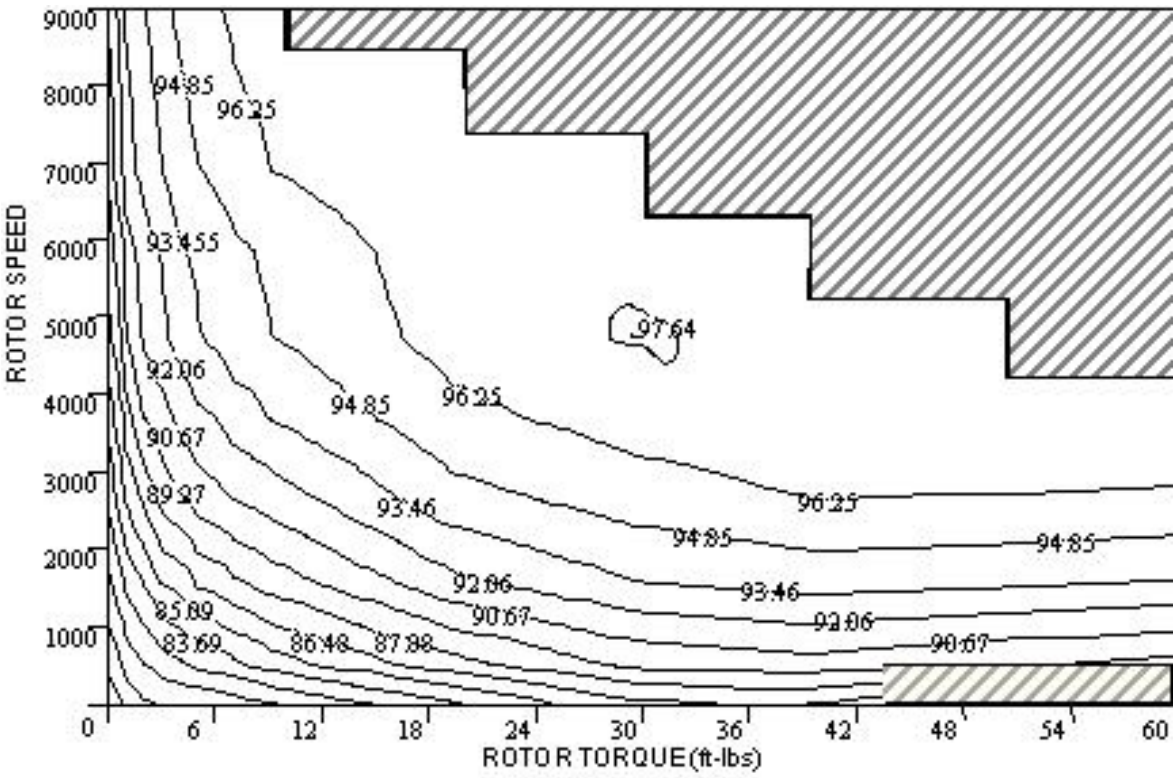

Figure 34: Soft-Switch Inverter Efficiency

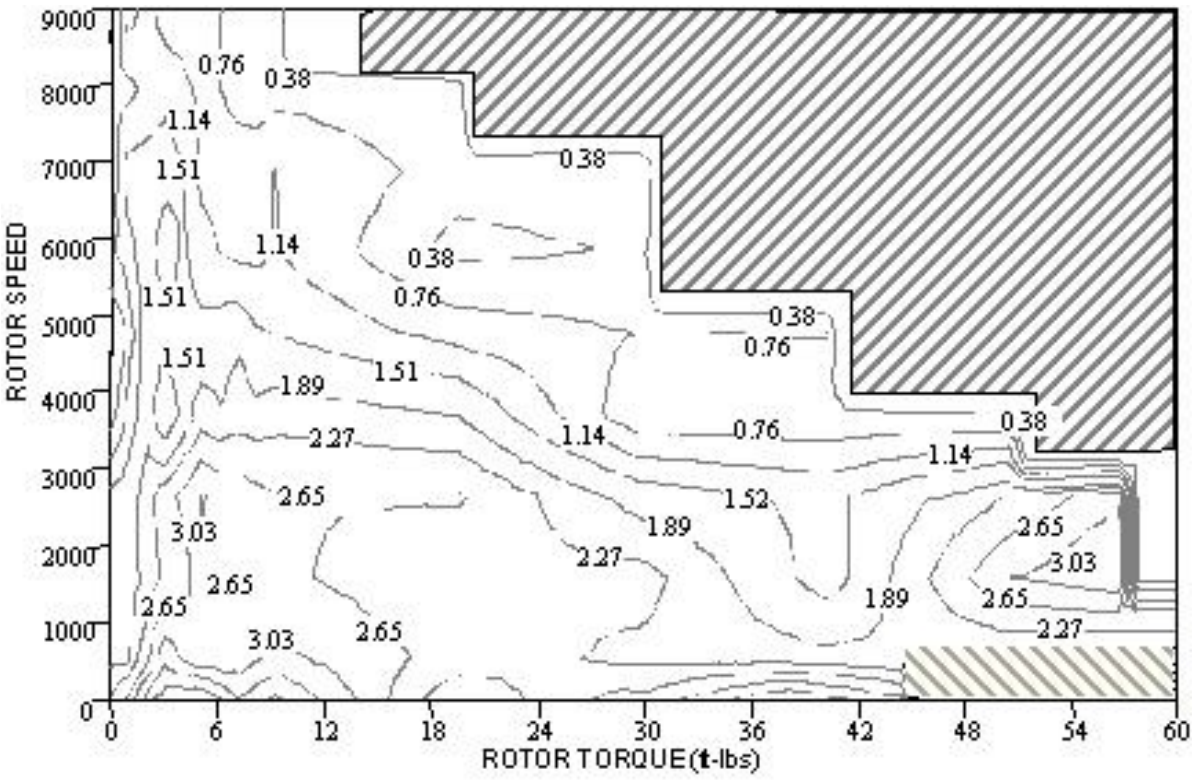

Figure 35: Soft Switching Efficiency Improvement

The next series of plots shows the impact of soft-switching on motor efficiency. The first plot shows the baseline motor efficiency under operation with the hard-switched EV2000. (Figure 36) The next efficiency plot shows the difference of the two motor efficiencies. (Figure 37) Finally, the total system efficiency of the hard switched inverter and motor is calculated. (Figure 38)

Note that the efficiency at light torque is difficult to measure accurately. (Figure 39) This is mostly attributed to offset error and noise pickup in the torque transducer hardware. At light torque (i.e.-25 – 150in-lb.), the torque transducer signal-to-noise ratio is low. This causes error between ± 5 - 10 % for light-load motor efficiency calculations. This error drops as the torque signal increases and remains below 1% for most of the data points collected on the motor.

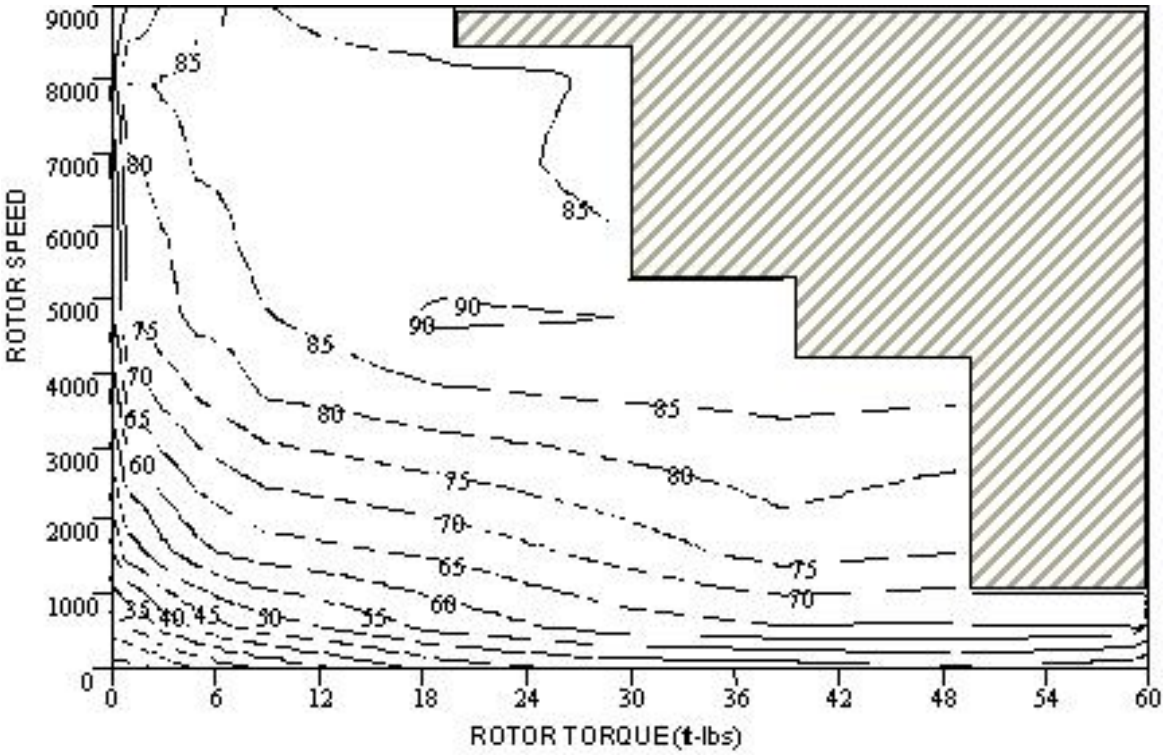

Figure 36: Motor Efficiency (EV2000 Hard-switched.)

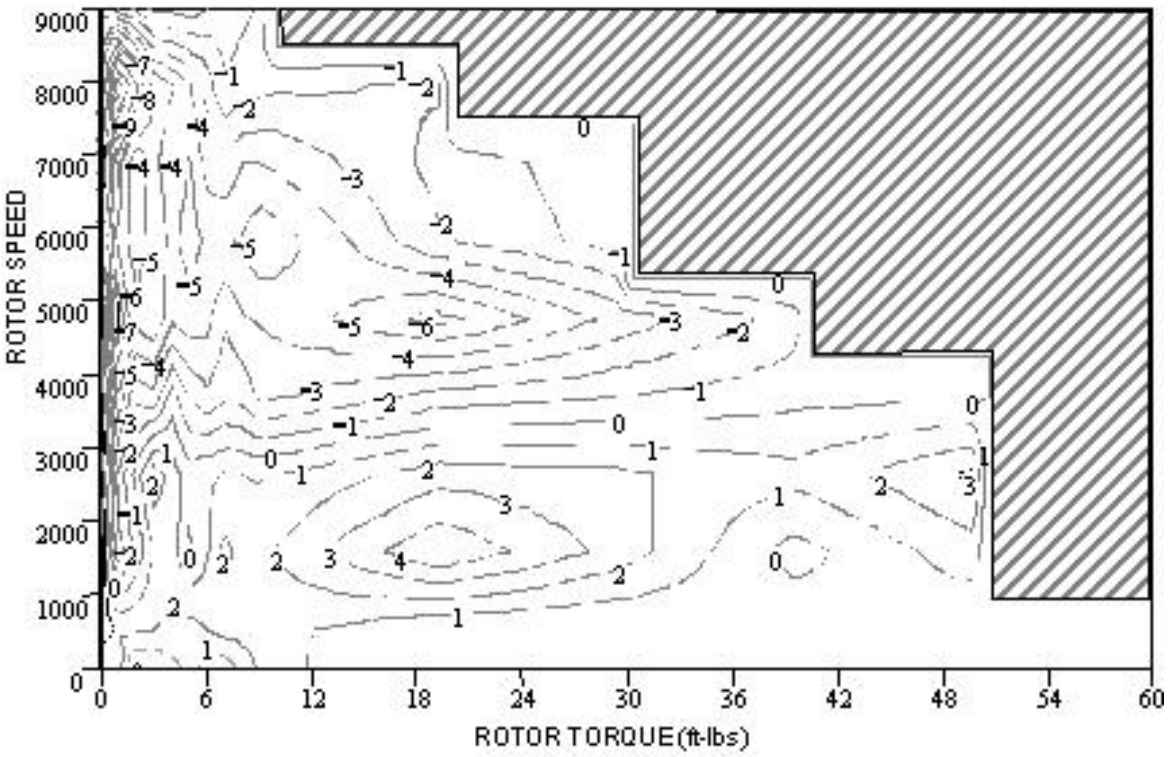

Figure 37: Motor Efficiency Difference (EV2000 Soft-switched.)

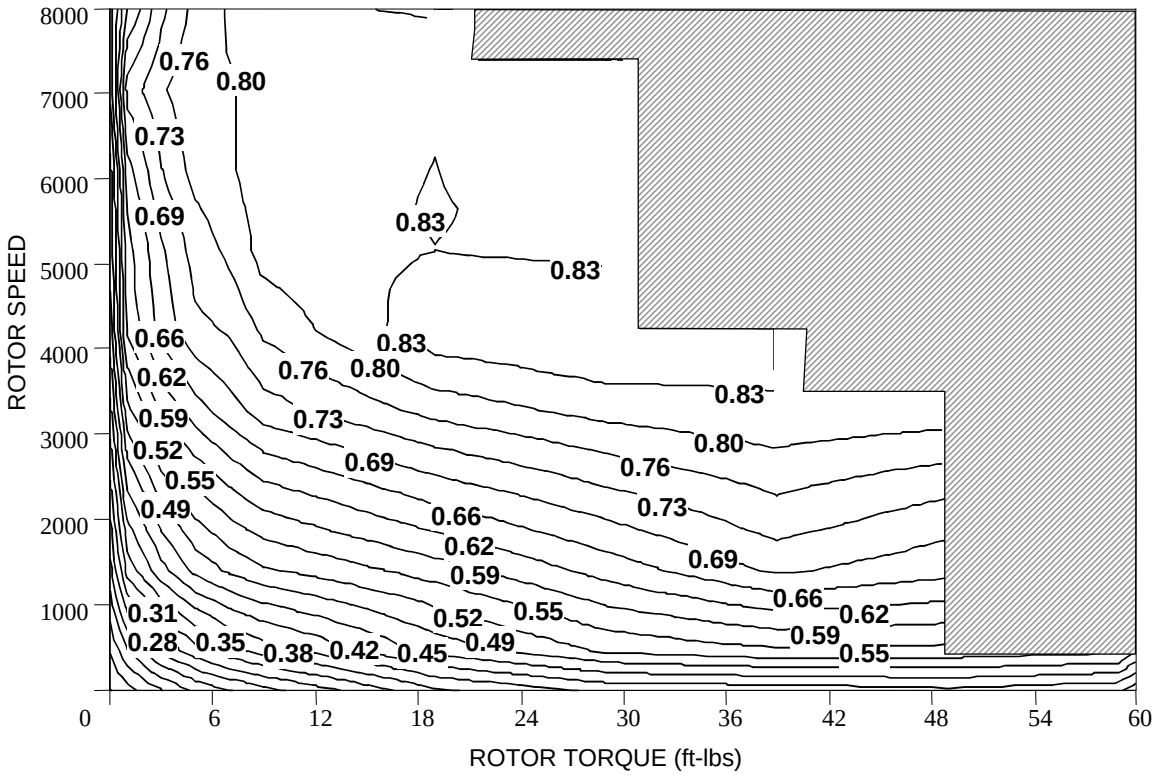

Figure 38: Hard Switched Hysteresis Controlled System Efficiency

6. 1. 2. DYNAMIC TEST RESULTS: FUDS CYCLE

The following FUDS cycle test results demonstrate the efficiency differences between a hard-switched and a zero-voltage-switched EV2000 inverter. Each test cycle is 12.0 km (7.45 mi.) and takes 1371 seconds to complete. Four FUDS test cycles were run on each inverter configuration for a total test time of 1 hour and 52 minutes. A five minute pause was inserted between each cycle to provide time for data compiling. The group of four tests was chosen to provide a sufficient time for the motor temperature to stabilize. This temperature reached 60 Celsius before the final FUDS test and moved 2 degrees above or below that number over the course of subsequent tests. For each test, six channels of data were collected at a rate of four times per second. These channels were:

1. DC input and AC output watts
2. Shaft output torque and speed
3. Motor and controller temperature

The results for FUDS cycle energy use were compiled with the built-in integrator of the power analyzer and post-processed from the data collection system. The efficiency results were available immediately after each test. These results were helpful in determining the amount of repeatability between FUDS tests. The results for the four FUDS cycles are shown in the following table.

Table 4: FUDS Drive Cycle Test Results for Hard and Soft Switching

Federal Urban Drive Schedule: Hard-Switched EV2000 Inverter				
Test Number	1	2	3	4
KWhr *In*	1.859	1.848	1.831	1.816
KWhr *Out*	1.625	1.619	1.602	1.602
Efficiency	87.4 %	87.6 %	88.0 %	88.2 %
Motor Temp	46 ºC	56 ºC	59 ºC	61 ºC
Soft-Switched EV2000 Inverter				
KWhr *In*	1.803	1.777	1.769	1.765
KWhr *Out*	1.616	1.603	1.598	1.597
Efficiency	89.6 %	90.2 %	90.4 %	90.5 %
Motor Temp	46 ºC	57 ºC	60 ºC	62 ºC
Difference in efficiency	2.2	2.6	2.4	2.3
Average eff. Hard-Switch	87.8 %			
Average eff. Soft-Switch	90.2 %			
% increase	2.75 %			

The cycle results show little variation from one another, however inverter efficiency rises 0.58% from tests 1-2, 0.24% from tests 2-3, and 0.10% from tests 3-4. Motor temperature rises 12C from tests 1-2, 5C from tests 2-3, and 3C from tests 3-4. A

simple proportional relationship between motor temperature and inverter efficiency is immediately visible. This seems to be caused by rotor heating that reduces the stator current required to develop the same shaft output torque.

6. 1. 3. DYNAMIC TEST RESULTS: HIGHWAY CYCLE

The following HIGHWAY cycle test results continue with the hard-switched and soft-switched EV2000 inverter. Each highway test cycle is 16.5 km (10.3 mi.) and takes 765 seconds to complete. Four highway test cycles were run on each inverter configuration for a total test time of 1 hour and 6 minutes. A five-minute pause exists between each cycle. The group of tests provide sufficient time for the motor temperature to stabilize at 57 Celsius just before the final highway test. No more than 2 degrees of temperature drift were observed after the complete warm-up.

The results for highway-cycle energy use were compiled with the built-in integrator of the power analyzer and post-processed from the data collection system.

Table 5: HWFET Drive Cycle Test Results for Hard and Soft Switching

Federal Highway Fuel Economy Test: Hard-Switched EV2000 Inverter				
Test Number	1	2	3	4
KWhr *In*	1.470	1.459	1.454	1.449
KWhr *Out*	1.334	1.338	1.334	1.334
Efficiency %	90.7	91.7	91.7	92.0
Motor Temp	44 ºC	51 ºC	55 ºC	58 ºC
Soft-Switched EV2000 Inverter				
KWhr *In*	1.444	1.438	1.429	1.425
KWhr *Out*	1.340	1.340	1.328	1.325
Efficiency %	92.8 %	93.2 %	92.9 %	92.9 %
Motor Temp	38 ºC	48 ºC	54 ºC	57 ºC
% increase in efficiency	2.28	1.62	1.3	0.97

Average eff. Hard-Switch	91.5 %
Average eff. Soft-Switch	93.0 %
% increase	1.64 %

6.2. Modulation Algorithm: Current Hysteresis Control vs. SVM

6. 2. 1. STEADY STATE TEST RESULTS

This section introduces the comparison of the effect of modulation changes on steady state efficiency. The steady state data covers both the inverter and motor. Steady state data is shown using contour plots. The first plot shows the base-line hard-switched RA-94 inverter. (Figure 39) This is followed by a plot that displays inverter efficiency difference. (Figure 40)

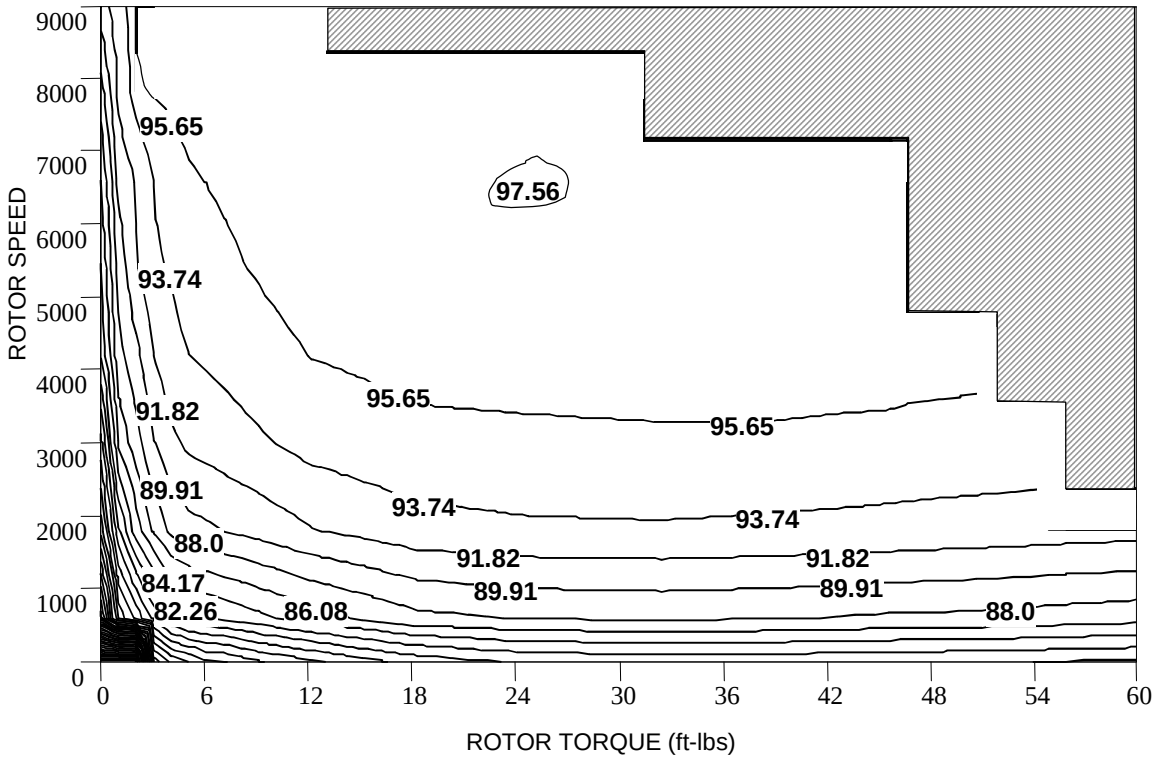

Figure 39: SVM Inverter Efficiency

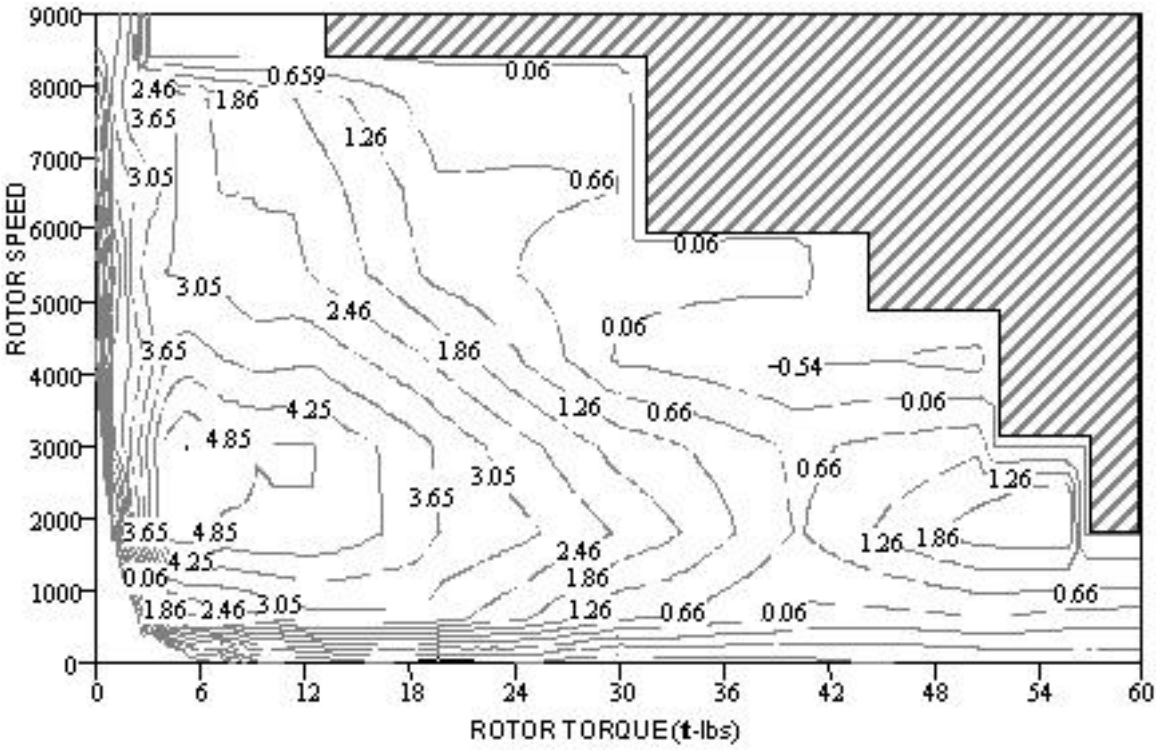

Figure 40: Efficiency Difference: SVM and Current Band Hysteresis Inverter (Hard-switched)

The next series of plots shows the impact of SVM on motor efficiency. It is expected that SVM will have a significant effect on motor harmonics and thus efficiency.[10] For this reason, the motor efficiency plot is shown as a difference of the motor efficiency between SVM and hysteresis control. (Figure 41) Notice that a wide range of improved efficiency especially at lower power levels. This large difference can only partly be attributed to measurement error, the efficiency difference far exceeds the 5-10 % range in the sensitive regions.

Further evidence in favor of increased motor efficiency is shown by operating temperature. A difference of 15 - 20ºC in motor temperature was recorded between steady state measurements taken with the SVM and hysteresis inverter.

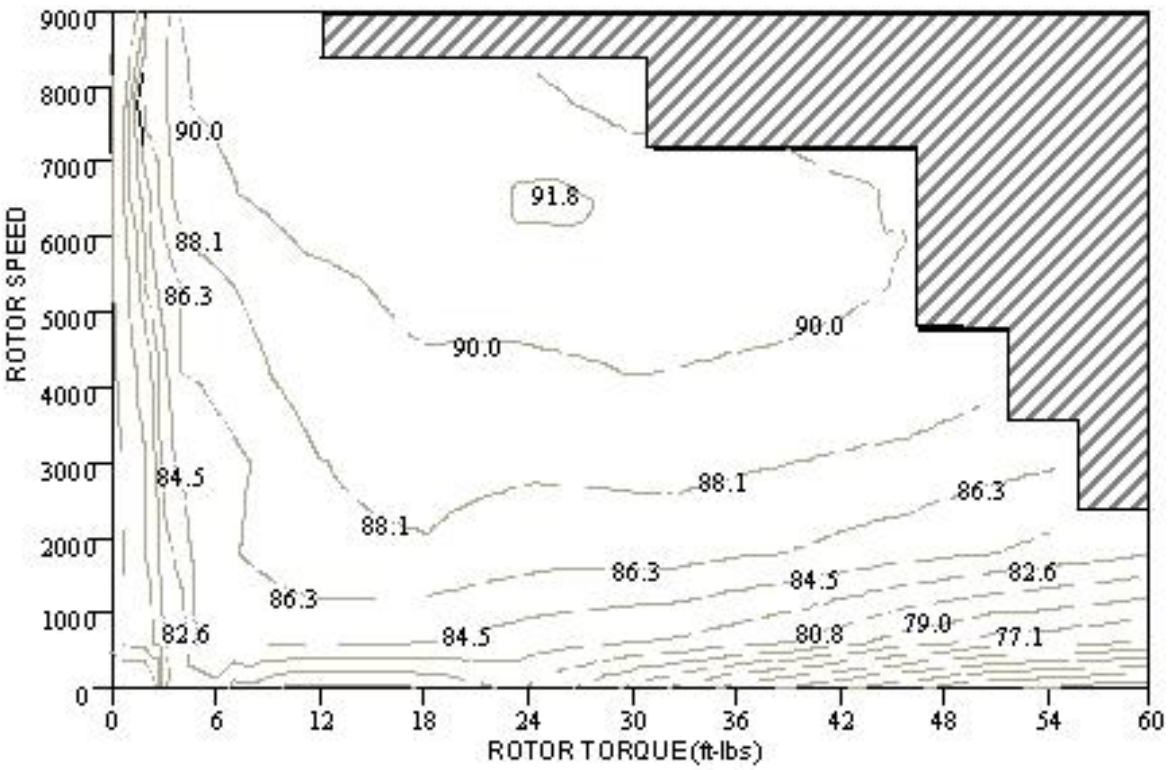

Figure 41: Motor Efficiency under the SVM Inverter

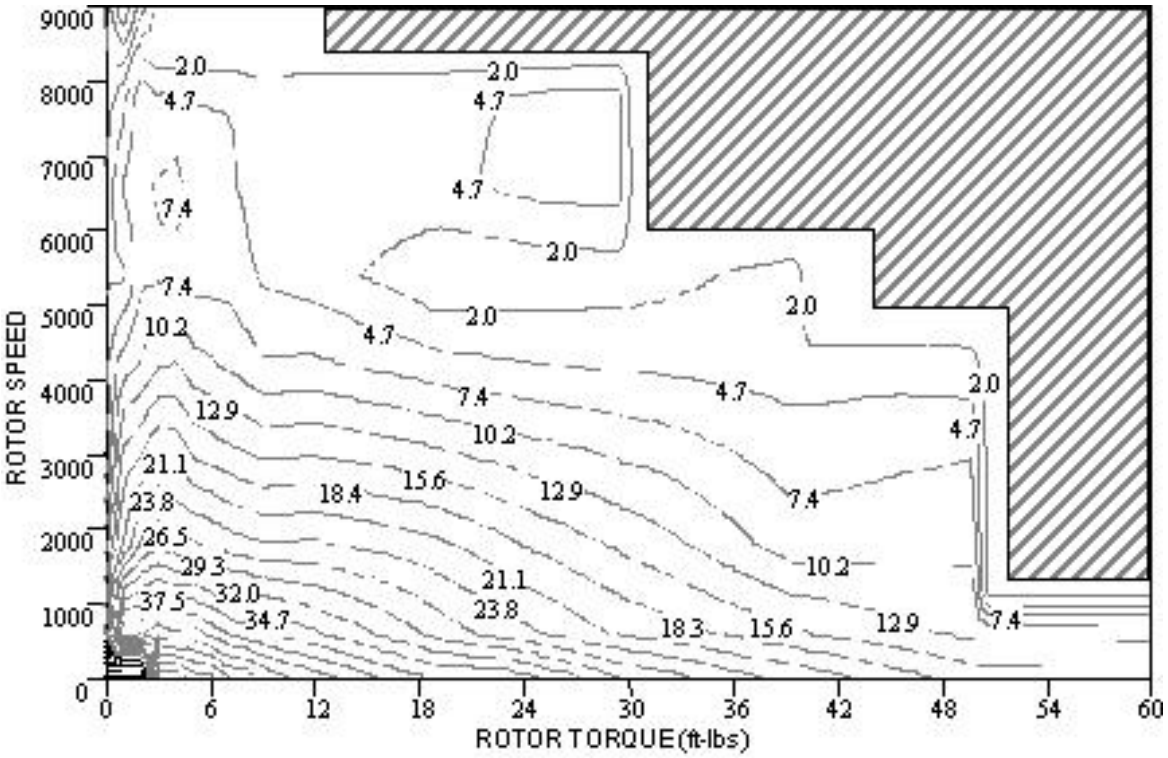

Figure 42: Motor Efficiency Improvement (SVM – Current Band Hysteresis)

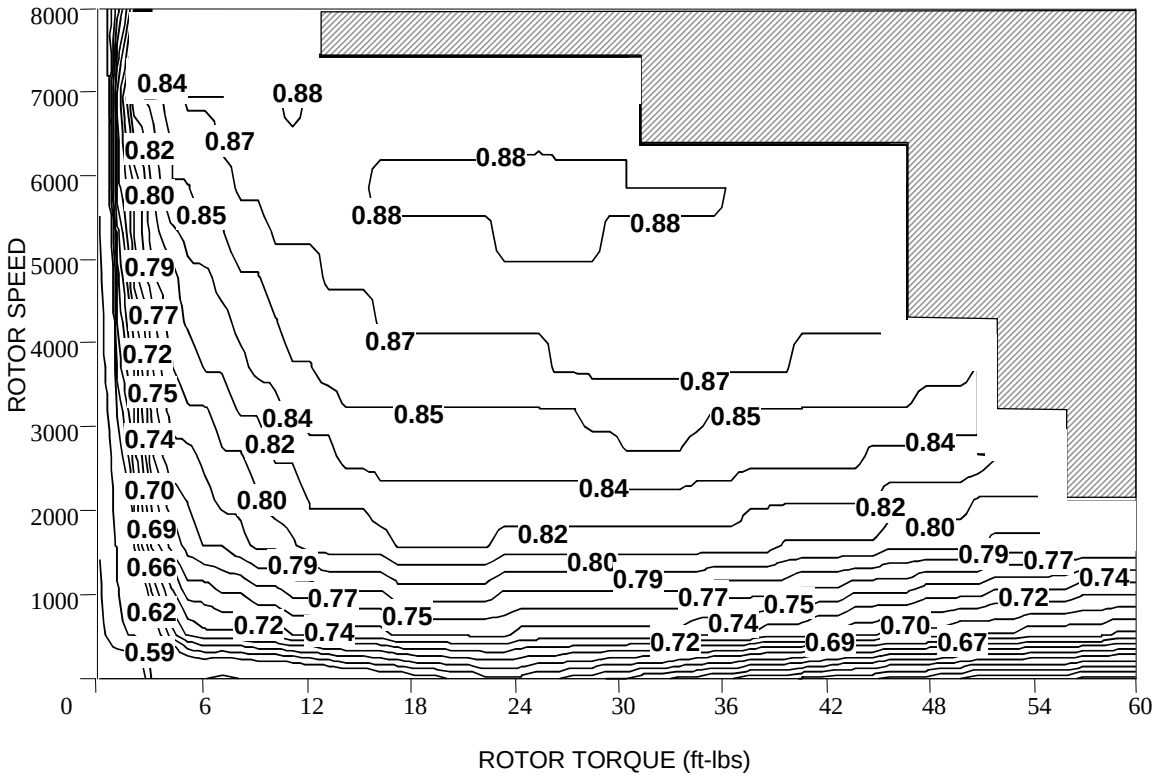

Figure 43: System Efficiency, SVM Hard Switched System

6. 2. 2. DYNAMIC TEST RESULTS: FUDS CYCLE

The following FUDS cycle test results demonstrate the efficiency differences between a hard-switched EV2000 and a hard-switched RA94 inverter. Each test cycle is 12.0 km (7.45 mi.) and takes 1371 seconds to complete. Four FUDS test cycles were run on each inverter configuration for a total test time of 1 hour and 52 minutes.

Motor temperature stabilized at 45 ºC before the final FUDS test and moved 2 degrees above or below that number over the course of subsequent tests.

Table 6: FUDS Drive Cycle Test Results for Modulation Algorithm Change

Federal Urban Driving Schedule: **Hard-Switched EV2000 Inverter, Hysteresis**				
Test Number	1	2	3	4
KWhr *In*	1.859	1.848	1.831	1.816
KWhr *Out*	1.625	1.619	1.602	1.602
Efficiency	87.4 %	87.6 %	88.0 %	88.2 %
Motor Temp	46 ºC	56 ºC	59 ºC	61 ºC
Federal Urban Driving Schedule: **Hard Switched RA-94 Inverter, SVM**				
KWhr *In*	1.533	1.542	1.542	1.542
KWhr *Out*	1.396	1.406	1.407	1.408
Efficiency	91.0 %	91.2 %	91.27 %	91.3 %
Motor Temp	35 ºC	41 ºC	44 ºC	45 ºC
Difference in efficiency	3.6	3.6	3.3	3.1
Average eff. : **Hysteresis**	87.8 %			
Average eff. : **SVM**	91.2 %			
% eff. Increase	3.86 %			

6. 2. 3. DYNAMIC TEST RESULTS: HIGHWAY CYCLE

The following HIGHWAY cycle test results continue with the hard-switched EV2000 and hard-switched RA-94 inverter. Each highway test cycle is 16.5 km (10.3 mi.) and takes 765 seconds to complete. Four highway test cycles were run on each inverter configuration for a total test time of 1 hour and 6 minutes. A five-minute pause exists between each cycle as in the FUDS cycles. The group tests provide sufficient time for the motor temperature to stabilize at 50 ºC just before the final highway test. No more than 2 degrees of temperature drift were observed after the complete warm-up.

The energy use results for the highway cycle were compiled with the built-in integrator of the power analyzer and post-processed from the data collection system similar to the FUDS test. The results for the four Highway cycles are shown in the following table.

Table 7: HWFET Drive Cycle Test Results for Modulation Algorithm Change

Federal Highway Fuel Economy Test: **Hard-Switched EV2000 Inverter, Hysteresis**				
Test Number	1	2	3	4
KWhr *In*	1.470	1.459	1.454	1.449
KWhr *Out*	1.334	1.338	1.334	1.334
Efficiency %	90.7	91.7	91.7	92.0
Motor Temp	44 ºC	51 ºC	55 ºC	58 ºC
Federal Highway Fuel Economy Test: **Hard-Switched RA-94 Inverter, SVM**				
KWhr *In*	1.444	1.438	1.429	1.425
KWhr *Out*	1.340	1.340	1.328	1.325
Efficiency %	95.2 %	95.1 %	94.9 %	95.0 %
Motor Temp	36 ºC	43 ºC	46 ºC	49 ºC
% increase in efficiency	4.5	3.4	3.2	3

Average eff. : **Hysteresis**	91.5 %
Average eff. : **SVM**	95.1 %
% eff. Increase	3.87 %

6.3.Topology: Soft-Switching vs. Hard Switching in an SVM Inverter

6. 3. 1. STEADY STATE TEST RESULTS: SVM WITH SOFT SWITCHING

The following plots detail the performance of the SVM inverter with ZVT soft-switching. Here, the soft-switched RA-94 inverter operates identical to the hard-switched configuration. The only difference is that the soft-switching components are physically connected to the bridge during the test. No changes are made to the fundamental control algorithm. Only small, fixed delay of 2.5 μs is added to the main switch signal from the inverter control processor.

The first plot shows inverter efficiency with soft-switching. (Figure 44) The next plot details the difference in efficiency between the soft and hard-switching versions of the same inverter. (Figure 44)

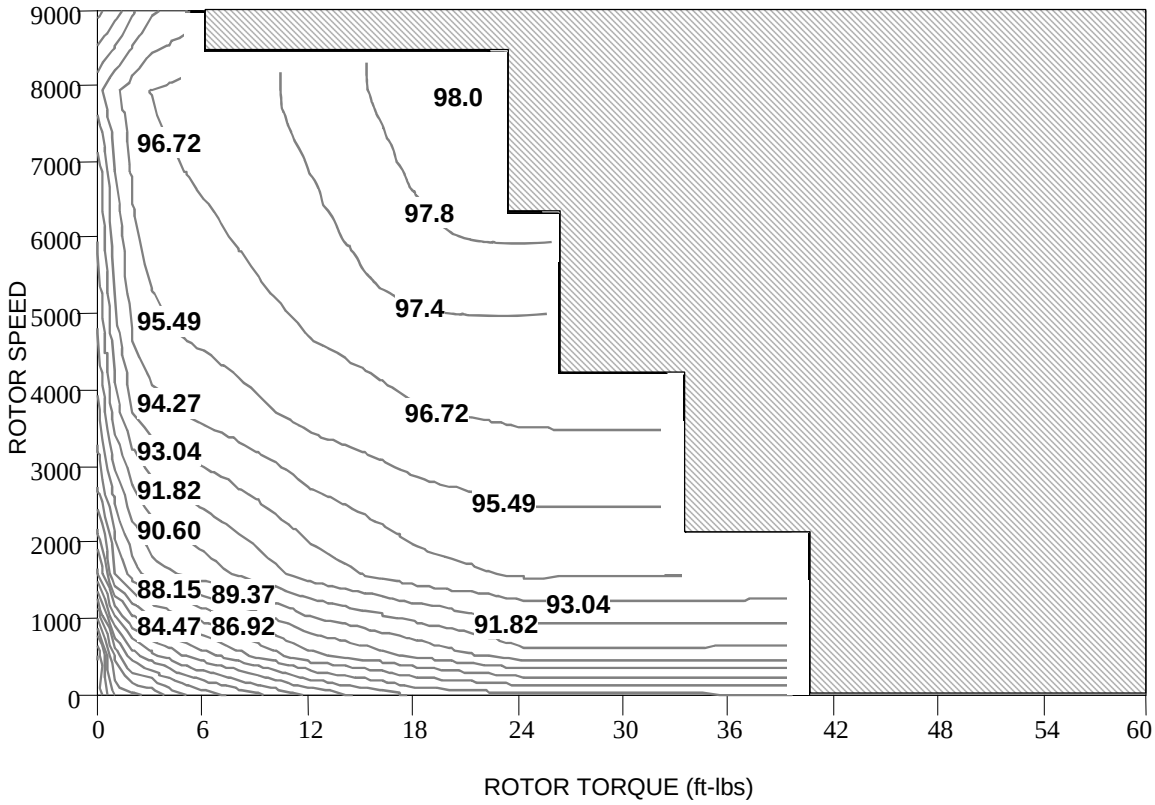

Figure 44: Inverter Efficiency for SVM with Soft-Switching

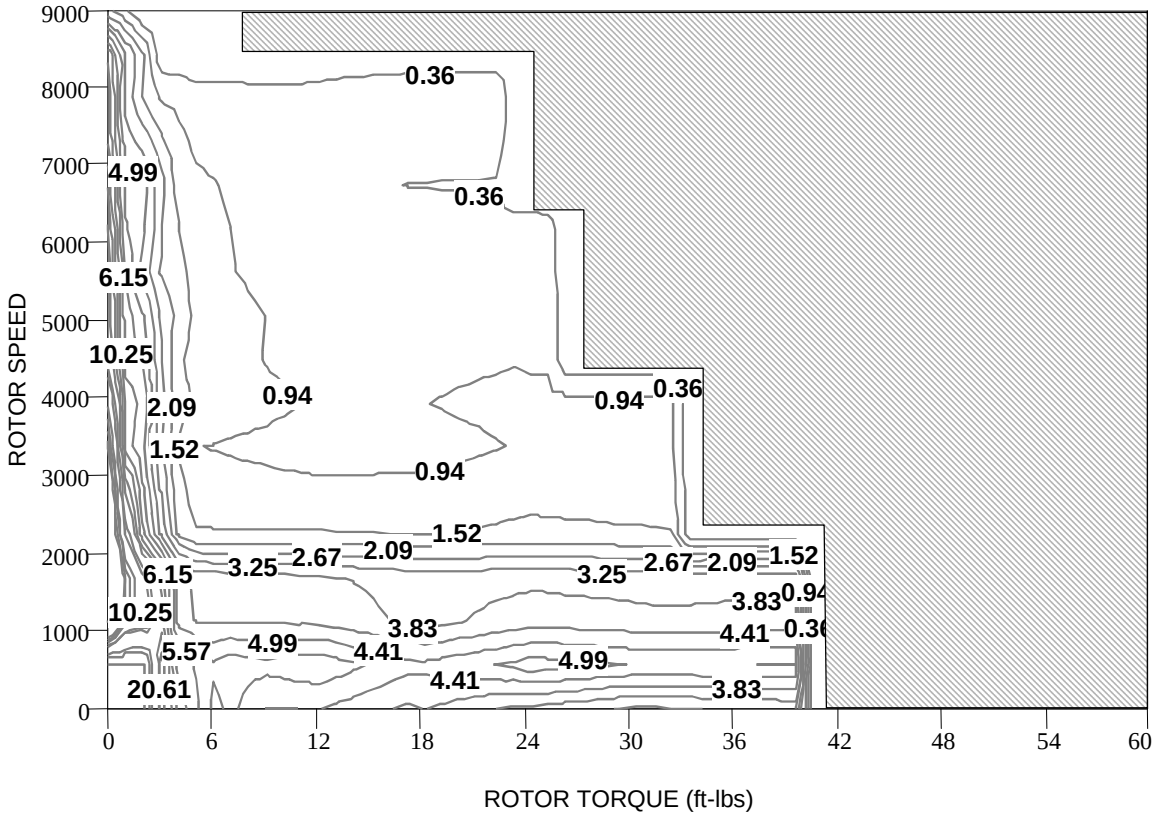

Figure 45: Inverter Efficiency Difference, (Soft and Hard-Switching SVM Inverter)

6. 3. 2. DYNAMIC TEST RESULTS: FUDS CYCLE, SVM SOFT AND HARD SWITCHING

The following FUDS cycle test results demonstrate the efficiency differences between a hard and soft-switched RA94 inverter. This temperature reached 45 ºC before the final FUDS test and moved within 2 degrees of that temperature over the course of subsequent tests.

HIGHWAY cycle test results compare soft and hard-switched RA-94 inverter. As with the previous tests four highway drive cycles are averaged to compare the two inverters.

Table 8: Comparison of Hard and Soft-Switching for an SVM inverter

Federal Urban Driving Schedule: **Hard-Switched RA-94 Inverter, SVM**				
Test Number	1	2	3	4
KWhr *In*	1.533	1.542	1.542	1.542
KWhr *Out*	1.396	1.406	1.407	1.408
Efficiency	91.0 %	91.2 %	91.3 %	91.3 %
Motor Temp	35 ºC	41 ºC	44 ºC	45 ºC
Federal Urban Driving Schedule: **Soft-Switched RA-94 Inverter, SVM**				
KWhr *In*	1.534	1.528	1.548	1.509
KWhr *Out*	1.406	1.408	1.406	1.399
Efficiency	91.7 %	92.1 %	90.8 %	92.7 %
Motor Temp	37 ºC	41 ºC	44 ºC	44 ºC
Difference in efficiency	0.7	0.9	-0.5	1.4
Average eff. : **Hard-Sw. SVM**	91.2 %			
Average eff. : **Soft-Sw. SVM**	91.8 % (92.2 %) excluding #3			
% eff. increase	0.66 % (1.1 %)			

6. 3. 3. DYNAMIC TEST RESULTS: HIGHWAY CYCLE

Table 9: Comparison of Hard and Soft-Switched Performance of an SVM Inverter

Federal Highway Fuel Economy Test: **Hard-Switched RA-94 Inverter, SVM**				
Test Number	1	2	3	4
KWhr *In*	1.444	1.438	1.429	1.425
KWhr *Out*	1.340	1.340	1.328	1.325
Efficiency %	95.2 %	95.1 %	94.9 %	95.0 %
Motor Temp	36 ºC	43 ºC	46 ºC	49 ºC
Federal Highway Fuel Economy Test: **Soft-Switched RA-94 Inverter, SVM**				
KWhr *In*	1.549	1.552	1.547	1.553
KWhr *Out*	1.476	1.480	1.478	1.486
Efficiency %	95.3 %	95.3 %	95.6 %	95.7 %
Motor Temp	34 ºC	43 ºC	48 ºC	50 ºC
Difference in efficiency	0.06	0.24	0.65	0.65
Average eff. : **Hard-Sw. SVM**	95.1 %			
Average eff. : **Soft-Sw. SVM**	95.45 %			
% eff. increase	0.36 %			

6.4.Results Summary

6.4.1. FUDS AND HIGHWAY CYCLE

The repeatability of the drive cycle tests was excellent. Between tests of topology, the variability was always within one percent torque for all tests. Also there was no perceptible difference between energy input and output over a range on tests. For drives with different modulation schemes, the FUDS cycle test was calibrated within one percent. The highway test was calibrated to within one percent for average torque and five percent for peak torque. This variation was due to the improvements in torque loop control. This is mainly due to the floating-point calculations done in the Analog Devices 2181 processor. The Texas Instruments processor used in the hysteresis inverter was a fixed-point processor. Both processors were able to faithfully recreate the load profiles as quickly as were commanded by the dynamometer computer.

In order to compare different inverters and motors, it is essential that the torque profiles show the same shape and magnitude. If these profiles are equivalent, then the energy used to generate these profiles can be used to judge efficiency. On this dynamometer, the torque profiles are always executed correctly. However, all drive cycle tests show a predictable decrease in motor current as the motor heats. In a vehicle, the driver observes this reduced torque and increases the torque command as necessary to offset this difference in acceleration. On the dynamometer, this thermal correction is not present. Therefore the speed profile remains correct, but torque production may fall. The drive is usually expected to automatically compensate for this, however about 5% drift can still occur after compensation.

This problem is corrected in the drive cycle program by multiplying the torque command by a correction factor so that the average torque of four drive cycles equal one nominal drive cycle. The result is an average of four test sessions that are used to derive drive cycle performance.

7. CONCLUSIONS

7.1.1. TOPOLOGY CHANGE: EV2000, HARD AND SOFT SWITCHING

The improvement due to soft-switching is easily observed from the steady state plots. Specific improvement exists in the low power areas of inverter operation. It is here that switching loss dominates because duty cycles remain low and switching frequency is high. Soft switching helps to eliminate most of the turn-on losses and impacts the inverter efficiency as detailed in the drive cycle summary below.

- FUDS efficiency improvement 87.8 % $\rightarrow$ 90.2 % = 20 % improvement
- Highway efficiency improvement 91.5 % $\rightarrow$ 93.0 % = 18 % improvement

The EV2000 enjoys at least an 18 % reduction in losses when soft-switching is enabled. This allows the inverter to operate in larger vehicles without the danger of increasing IGBT stress. Better reliability and performance is expected in the motor. This is because soft-switching reduces the high rate of rise in voltage that is a source of parasitic current flow in motors.

Motor efficiency is also affected by soft-switching, however it is no more than 6% in this inverter. At low rotor speeds, motor efficiency is slightly higher for the soft-switched inverter. However, the opposite is true at high rotor RPM. This would mean that the overall system efficiency is roughly balanced out when operated at both low and high power.

7.1.2. MODULATION CHANGE: EV2000 AND RA-94 HARD SWITCHING

The improvement due to modulation change is evident from the steady state plots. At almost all power levels, a consistent efficiency gain exists. This is especially true at low power operation over the entire tested RPM range. It is here that switching losses are reduced because of optimal zero vector selection made by the modulator circuit. The

impact of modulation algorithm on inverter efficiency as detailed in the drive cycle results shown below.

- FUDS 87.8 % → 91.2 % = 28 % improvement
- Highway 91.5 % → 95.1 % = 42 % improvement

By far the most impressive results for this thesis are realized by the motor efficiency improvement. This is due to the low distortion waveforms created by the SVM modulator. The motor efficiency improvement provides an immediate decrease in temperature measured at the stator. The temperature rise after four drive cycle tests was usually half of that measured when using the hysteresis inverter for the same test. This gives the motor designer freedom to either decrease the size of the oil cooling system, or use a simple, cheaper air cooled stator.

7.1.3. TOPOLOGY CHANGE: RA-94 HARD-SWITCHED AND RA-94 SOFT SWITCHED

Soft-switching was also implemented on the SVM inverter. This soft-switched inverter showed improvement over a wider range of torque and speeds than did the hysteresis inverter. This is mostly due to the constant 10 kHz switching frequency. However, soft-switching benefits on this inverter are not as dramatic. This is because the most advantageous soft-switching events (at maximum current) do not occur when using an intelligent zero vector SVM technique. The correct selection of zero vectors allows the IGBT handling the highest current to stay closed. This eliminates up to half of the switching losses even without soft-switching.

- FUDS 91.2 % → 92.2 % = 11 % improvement
- Highway 95.1 % → 95.45 % = 7 % improvement

Motor efficiency is expected to be the same for both configurations of the drive. The addition of soft-switching would mainly benefit the reliability of the motor. This is because ZVT circuits reduce motor damage caused by excessive dv/dt during IGBT turn-on. ZVT circuits can also allow safe inverter operation at increased switching frequency. This permits the inverter to create less damaging motor harmonics.

Summary of Drive Cycle Results:

When a soft-switched inverter is used:

- Turn-on losses and diode reverse recovery problems are virtually eliminated.
- Up to 20% energy improvement may be seen
- Motor efficiency remains essentially unchanged
- Turn-off snubbers can be used to help eliminate turn-off loss
- Increased cost and volume due to added device hardware

When modulation algorithm is changed:

- SVM helps eliminate a large amount of switching losses.
- Current waveforms are free of damaging harmonics that impact the motor and the conduction losses of inverter.
- Motor efficiency is dramatically better than current-band hysteresis
- More complex software implementation required

The following bar graph summarizes the efficiency results of all the different configurations. From this graph, it seems that the best choice would be the hard-switched version of the SVM inverter. (Figure 46) The soft-switched version does have higher efficiency but the additional cost of the soft-switch circuit may not be justified. This is because the additional increase in efficiency would have a minimal impact on overall efficiency.

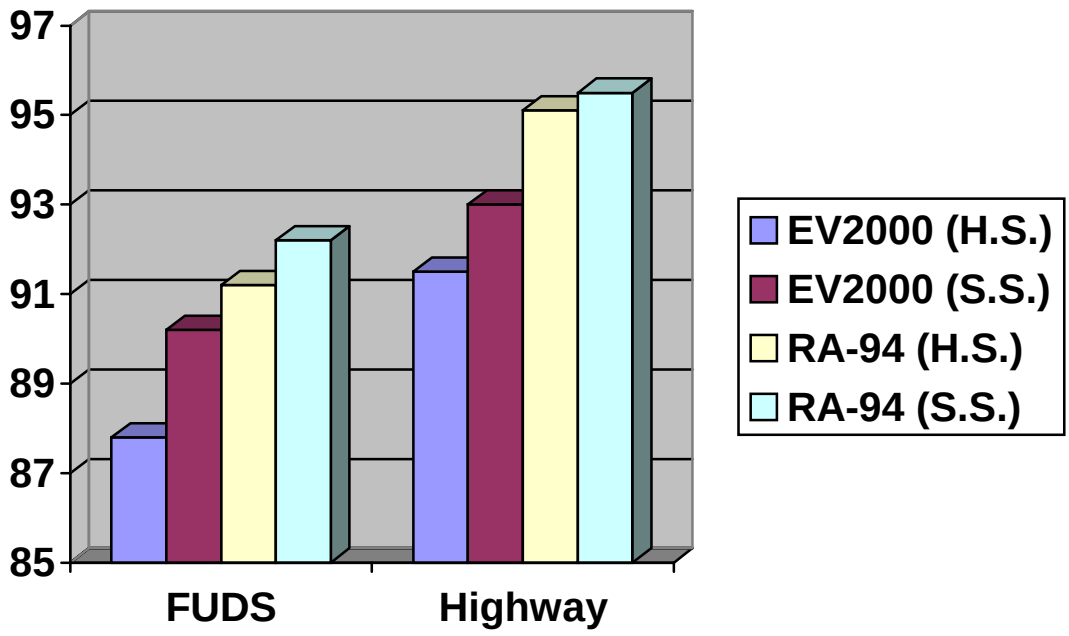

Figure 46: Drive Cycle Efficiency Improvement Summary

7.1.4. General Conclusions

The dynamometer test platform provides an accurate evaluation of inverter and motor efficiency for a wide range of steady state and dynamic operating points. The platform combines automatic control with data logging of mechanical and electrical power.

Dynamic drive cycle testing of inverters can be accomplished through the drive cycle generator and drive cycle player. The drive cycle generator provides a complete platform for modifying drive cycles or using industry standard files. The parameters of the target vehicle are configured and then the program solves a differential equation to calculate and create a control file. This control file contains the torque and speed commands required to run the drive cycle test. The drive cycle player then decodes the data file and sends the appropriate commands to the torque and speed control inverters. Using delay logic, the drive cycle player allows the user to fine-tune the timing of drive cycle execution so that it runs for the correct amount of time.

All the data collected from steady state and dynamic testing must illustrate the benefits possible when an inverter topology or modulation algorithm is changed. Steady state efficiency plots are able to show the actual effects of a design change at any particular point. Drive cycle analysis takes the improvements and puts them in action, magnifying the benefits or detriments of a design change. An example of benefits is the soft-switching results in the FUDS drive cycle test. An increase in inverter efficiency of 2.75 percent for a normal daily commute might offer negligible 1.2 miles of increased range. However, this inverter efficiency improvement cuts losses by 20 percent. This can have a direct and substantial impact on heatsink size requirements and/or inverter rating.

The dynamometer testbed fulfills its purpose of providing a tool for evaluation of electric drive performance. As with any good tool, this system can be expanded to control a variety of drive systems through a variety of available communications links. The testbed offers expandability and versatility in a manner that allows an operator to adapt this tool to a variety of drive systems. Therefore, it can evolve along with newer drive technology to continue supporting electric vehicle research.

REFERENCES

[1] De Doncker and J. P. Lyons, "The Auxiliary Resonant Commutated Power Converters", *in Conference Records of IEEE IAS 1990*, pp. 1228-1235.

[2] Ivo Barbi, D. C. Martins, "A True PWM Zero-Voltage-Switching Pole with Very Low Additional RMS Current Stress", *in Conference Records of IEEE PESC 1991*, pp. 261-267.

[3] Joel P. Gegner, C. Q. Lee, "Zero-Voltage-Transition Converters Using and Inductor Feedback Technique", *in proceedings of IEEE IPEC 1994*, pp. 862-868.

[4] S. Frame, S. Dubovsky, Q. Li, D. Katsis, C. Cuadros, D. Borojevic, F.C. Lee, "Three-Phase Soft-Switching Inverters for Electric Vehicle Applications", *in proceedings of VPEC Seminar '95*, pp. 45-52.

[5] S. Frame, D. Katsis, D. H. Lee, D. Borojevic, F.C. Lee, "A Three-Phase Zero-Voltage-Transition Inverter with Inductor Feedback", *in proceedings of VPEC Seminar '96*, pp. 189-193.

[6] R.W. Booth, "VPI Speed Regulator", General Electric Drive Systems, Salem VA, 10/12/95

[7] R.W. Booth, "MEVP Control Dictionary", ", General Electric Drive Systems, Salem VA

[8] Riley, R.Q.: Alternative Cars in the 21st century: A New Transportation Paradigm, *Society of Automotive Engineers, Inc.* copyright 1994.

[9] S. Frame, S. Dubovsky, Q. Li, C. Cuadros, D. Borojevic and F.C. Lee "Three Phase Soft-Switching Inverters for Electric Vehicle Applications" *VPEC Internal Publication*, Report made for Hughes Power Systems, 1994

[10] H.W. Van Der Broeck, H.C. Skudelny, and G.V. Stanke, “Analysis and Realization of a Pulse Width Modulator Based on Voltage Space Vector” IEEE Trans. On Ind. App., vol 24, no.1, pp 142-150, Feb. 1988

VITA

DIMOSTHENIS C. KATSIS

Work Address	**Permanent Address**
1501 Roanoke Boulevard	**1933 Windsor Ave. Apt. 4**
Salem, VA 24153	**Roanoke, VA 24015**
+1 (540) 387 8685	**+1 (540) 342 1373**

email: katsis-dc@salem.ge.com, dkatsis@vt.edu

Dimosthenis Katsis, son of Vasilios D. Katsis and Dina P. Katsis was born February 24, 1973 and raised in Winston-Salem, Forsyth County, North Carolina.

Dimos Katsis pursued studies in electrical engineering at Virginia Tech in 1991. This followed successful completion and graduation from the North Carolina School of Science and Mathematics in Durham, NC. Dimos's main interests focused on solar and electric vehicles during his entire academic career at Virginia Tech. The solar powered vehicle project provided teamwork and leadership opportunities in the fields of motor and power electronics. Dimos continued to lead and create a new engineering initiative, the Hybrid-Electric Vehicle Team of Virginia Tech, the leading university hybrid-electric vehicle research team in the nation.

Dimos Katsis graduated with his BSEE in May 1995, and remained at Virginia Tech to pursue his masters degree. He joined the Virginia Power Electronics Center (VPEC), the nation's top university-based power electronics research center. He immediately began work on a government-sponsored program to improve the cost and performance of electric vehicle motor drives. This research focused on development of soft-switching technology for the power semiconductors. Later research emphasized system development of the entire inverter drive system. Dimos designed and supervised the construction of a computer controlled motor dynamometer. This dynamometer was

used to evaluate the newly designed electric vehicle drive developed at VPEC. Dimos completed his work at VPEC and defended his thesis on August 27, 1997.

Dimos's research interests continue in the field of motor drives and motor control. Specific research has focused in the benefits of various efficiency improving techniques used in electric vehicles. Other research has focused on the application of alternative fuels to mass transit including compressed natural gas power systems.

Dimos Katsis presently holds a position in design engineering at General Electric in the Technical Leadership Program.

Education

1991: North Carolina School of Science and Mathematics, Durham, NC

B.S.E.E., May 1995: Virginia Polytechnic Institute and State University, Blacksburg, VA

M.S.E.E., December 1997: Virginia Polytechnic Institute and State University, Blacksburg, VA

Masters Thesis: Development of a Testbed for Evaluation of Electric Vehicle Drive Performance

Research and Work Experience

Virginia Power Electronics Center June 1995 – August 1997

- Research and Development of an Electric Vehicle Motor Controller
- Design And Implementation of a 75 Kilowatt Electric Motor Dynamometer Testing Laboratory
- Designed and Built Charger System for a Hybrid-Electric Vehicle

Assistant Engineer to Consulting Firm August 1995 – December 1996

- Designed Liquid Level Controller for Multiple Pump Installation and Non-Corrosive Water Level Measurement
- Research and Programming of Low Cost Embedded Microcontrollers

Hybrid-Electric Vehicle Project / Solar-Electric Vehicle Project

September 1991 - June 1995

- Electrical Team Leader for The Hybrid-Electric Vehicle Project (June 1994-June 1995)
- Supervised Design And Implementation of Electric Vehicle Drive, Hybrid Electric Control Strategy, AC-DC Conversion Research, and Total Vehicle System Integration
- Electrical Team Leader for Solar-Electric Vehicle Project (May 1992 - Jan. 1993)
- Designed and Constructed Solar Array Power Switching Units With Simple Adaptive Control for Maximum Power Tracking
- Battery Research Team Leader, Developed Testing Methods for Electric Vehicle Batteries and Models To Characterize and Predict Battery Performance

PUBLICATIONS

Primary Authorship:

1. D. C. Katsis, F.C. Lee, "A Single Buck Converter for Hybrid Vehicle Generators", *Proceedings of the Workshop on Power Electronics in Transportation*,1996 *pp. 117-125*
2. D. C. Katsis, M. Herwald, J. Choi, D. Borojevic, and F.C. Lee, "Drive Cycle Analysis of an Electric Vehicle Inverter", *in proceedings of IECON '97*, in press.
3. D. C. Katsis, "Development of a Testbed for the Evaluation of Electric Vehicle Drive Performance", Master's Thesis, *Virginia Polytechnic Institute and State University, 1997*

Contributing Authorship:

1. W. Stinnett, D. C. Katsis, "Design of the Virginia Tech Hybrid-Electric Vehicle", *Society of Automotive Engineers Journal of Hybrid-Electric Vehicles 1995*

2. S. Frame, D. C. Katsis, D. H. Lee, D. Borojevic, F.C. Lee, "Three-Phase Soft-Switching Inverters for Electric Vehicle Applications", *in proceedings of VPEC Seminar '95*, pp. 45-52.
3. S. Frame, D. C. Katsis, D. H. Lee, D. Borojevic, F.C. Lee, "A Three-Phase Zero-Voltage-Transition Inverter with Inductor Feedback", *in proceedings of the European Power Electronics Society '97*, in press.

ORGANIZATIONS AND AWARDS

Institute of Electrical and Electronic Engineers (IEEE), student branch member of the year 1994

American Society of Mechanical Engineers Technical Presentation Competition: First Place in Region 1992

Duracell/NSTA Scholarship 1991